

Lourdes Urda

Effective Field Theory Results from the CMS experiment

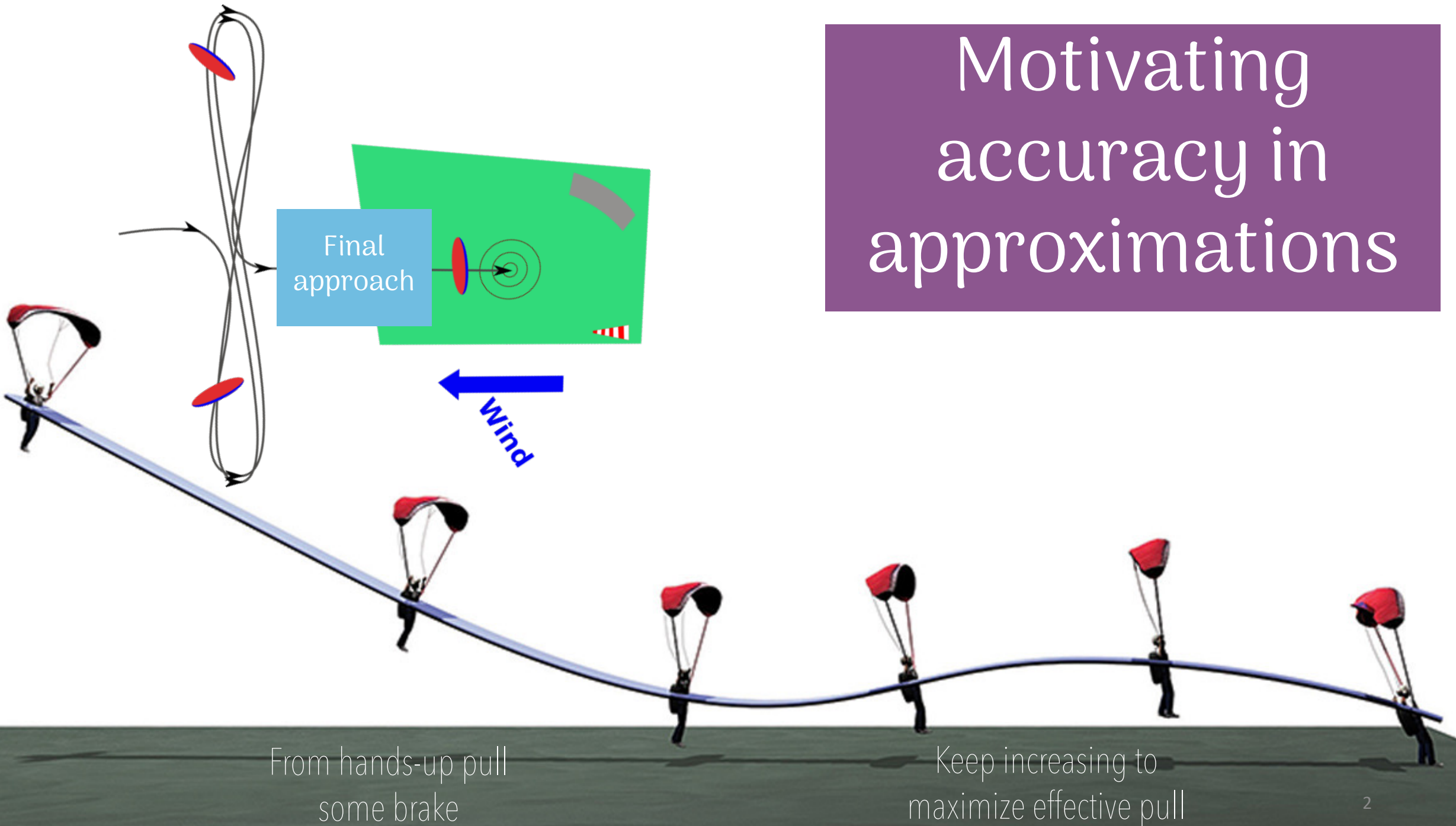


Higgs Hunting 2024



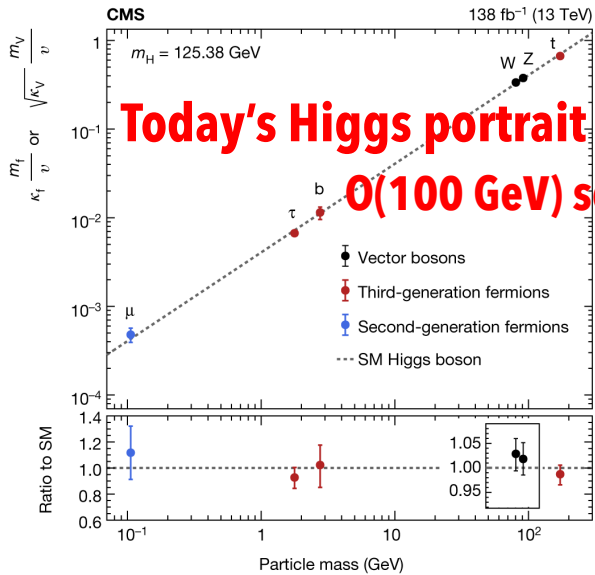
24/09/24

Motivating accuracy in approximations



STANDARD MODEL (SM)

Nature 607 (2022), 60-68



NEW PHYSICS (NP)

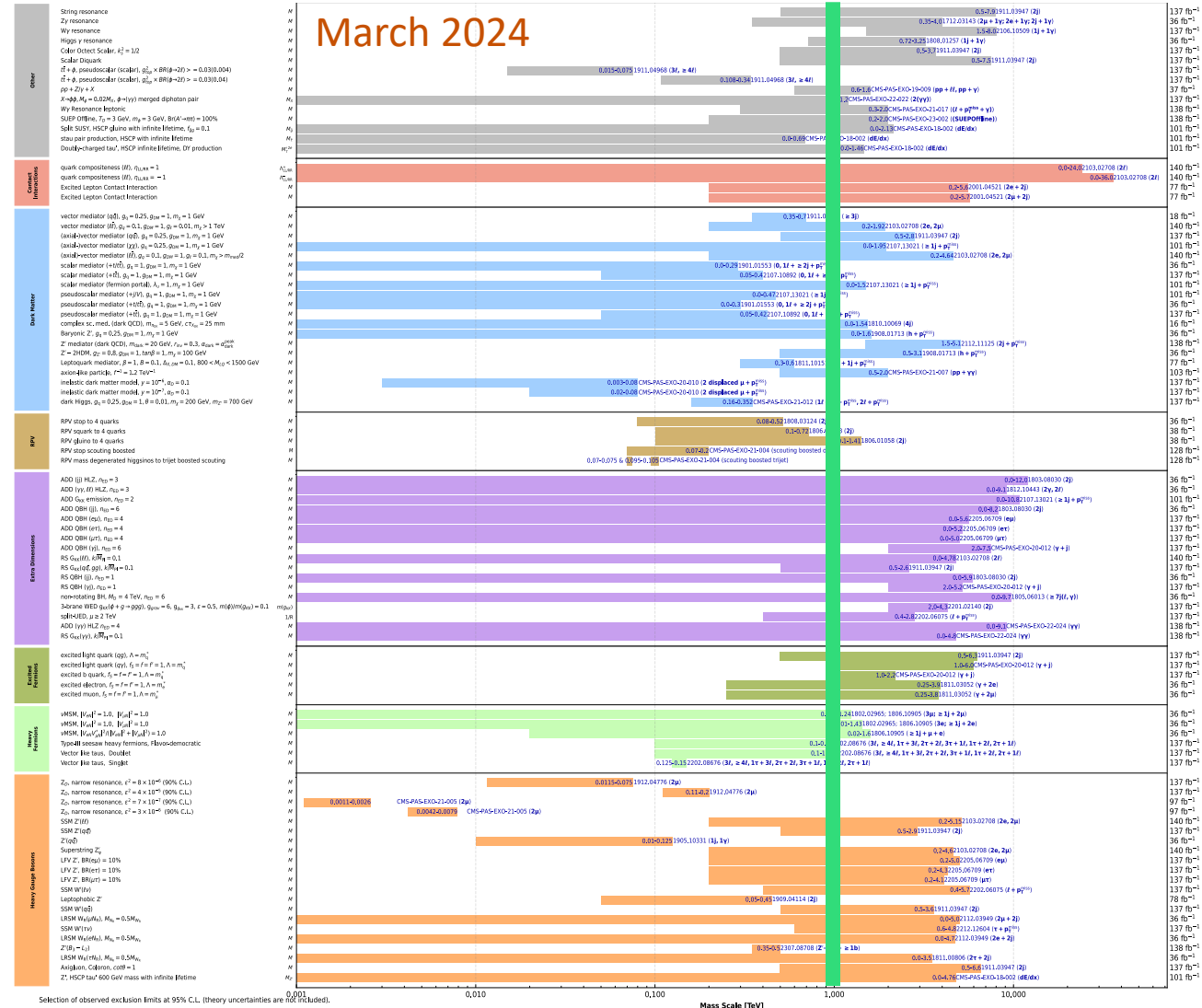
EFT

CMS analyses indicating an energy gap between SM physics and NP

EFT links phenomena across different energy scales

Overview of CMS EXO results

March 2024



Selection of observed exclusion limits at 95% C.L. (theory uncertainties are not included).

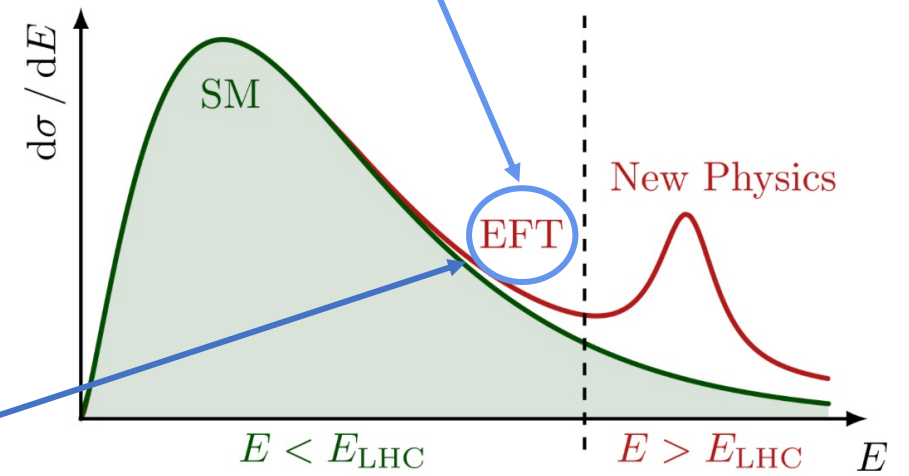
~1 TeV

SM Effective Field Theory (SMEFT)

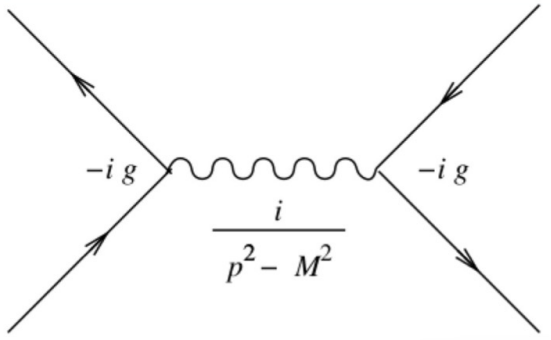
$$\mathcal{L}_{eff} = \mathcal{L}^{SM} + \mathcal{L}^{D=6}, \quad \mathcal{L}^{D=6} = \frac{1}{\Lambda^2} \sum_i c_i^{(6)} \mathcal{O}_i^{(6)}$$

- ✓ c_i specify the strength of the new interactions
- ✓ EFT only valid at $E < \Lambda$

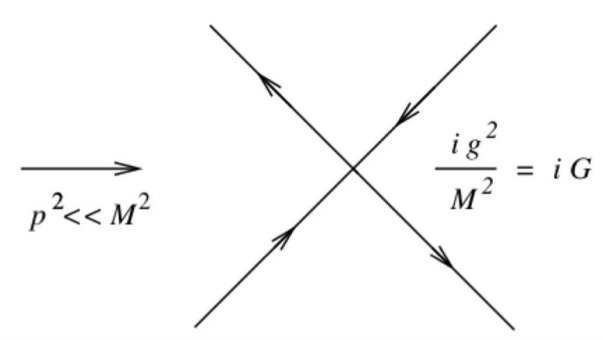
Deformations in SM described by $\mathcal{O}_i^{(6)}$ effective interaction



Full theory (New Physics)



Effective interaction (EFT)



Cross section (xs) also affected as:
 SM xs + SM-BSM interference xs + BSM xs

CMS analyses enable us to accurately place limits on Wilson Coefficients (c_i)

CMS Run 2 EFT-related analyses

Individual channels

$$H \rightarrow WW \rightarrow e\mu\nu\nu$$

[Eur. Phys. J. C 84 \(2024\) 779](#)

New!

$$VH \rightarrow bb$$

[CMS-PAS-HIG-23-016](#)

New!

$$HZ\gamma \text{ and } H\gamma\gamma$$

[CMS-PAS-HIG-23-011](#)

Combination of channels



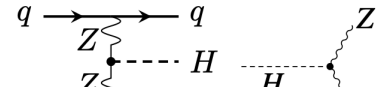
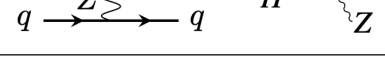
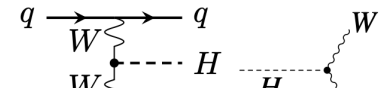
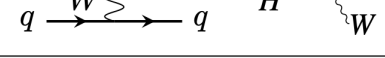
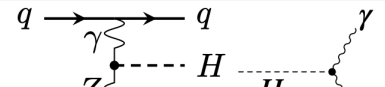
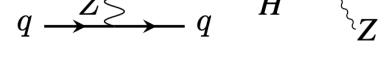
EFT interpretation of Higgs diff. fid. measurements

[CMS-PAS-HIG-23-013](#)

New!

EFT interpretation of SM measurements

[CMS-PAS-SMP-24-003](#)

Operator	Wilson coefficient	Example process
$H^\dagger H G_{\mu\nu}^a G^{a\mu\nu}$	c_{HG}	
$H^\dagger H \tilde{C}_{\mu\nu}^a G^{a\mu\nu}$	\tilde{c}_{HG}	
$H^\dagger H B_{\mu\nu} B^{\mu\nu}$	c_{HB}	
$H^\dagger H \tilde{B}_{\mu\nu} B^{\mu\nu}$	\tilde{c}_{HB}	
$H^\dagger H W_{\mu\nu}^i W^{i\mu\nu}$	c_{HW}	
$H^\dagger H \tilde{W}_{\mu\nu}^i W^{i\mu\nu}$	\tilde{c}_{HW}	
$H^\dagger \sigma^i H W_{\mu\nu}^i B^{i\mu\nu}$	c_{HWB}	
$H^\dagger \sigma^i H \tilde{W}_{\mu\nu}^i B^{i\mu\nu}$	\tilde{c}_{HWB}	

Global EFT data analyses are highly motivated

A single operator can influence many processes, and multiple operators can affect one single process.

H \rightarrow WW \rightarrow e μ $\nu\nu$

Based on likelihood ratios

$$D_{\text{BSM}} = \frac{\mathcal{P}_{\text{BSM}}(\vec{\Omega})}{\mathcal{P}_{\text{BSM}}(\vec{\Omega}) + \mathcal{P}_{\text{SM}}(\vec{\Omega})}$$

Reconstruction at detector-level

MELA-based kinematic discriminants
(KD) sensitive to production vertex:

Production mode (D_{VBF})

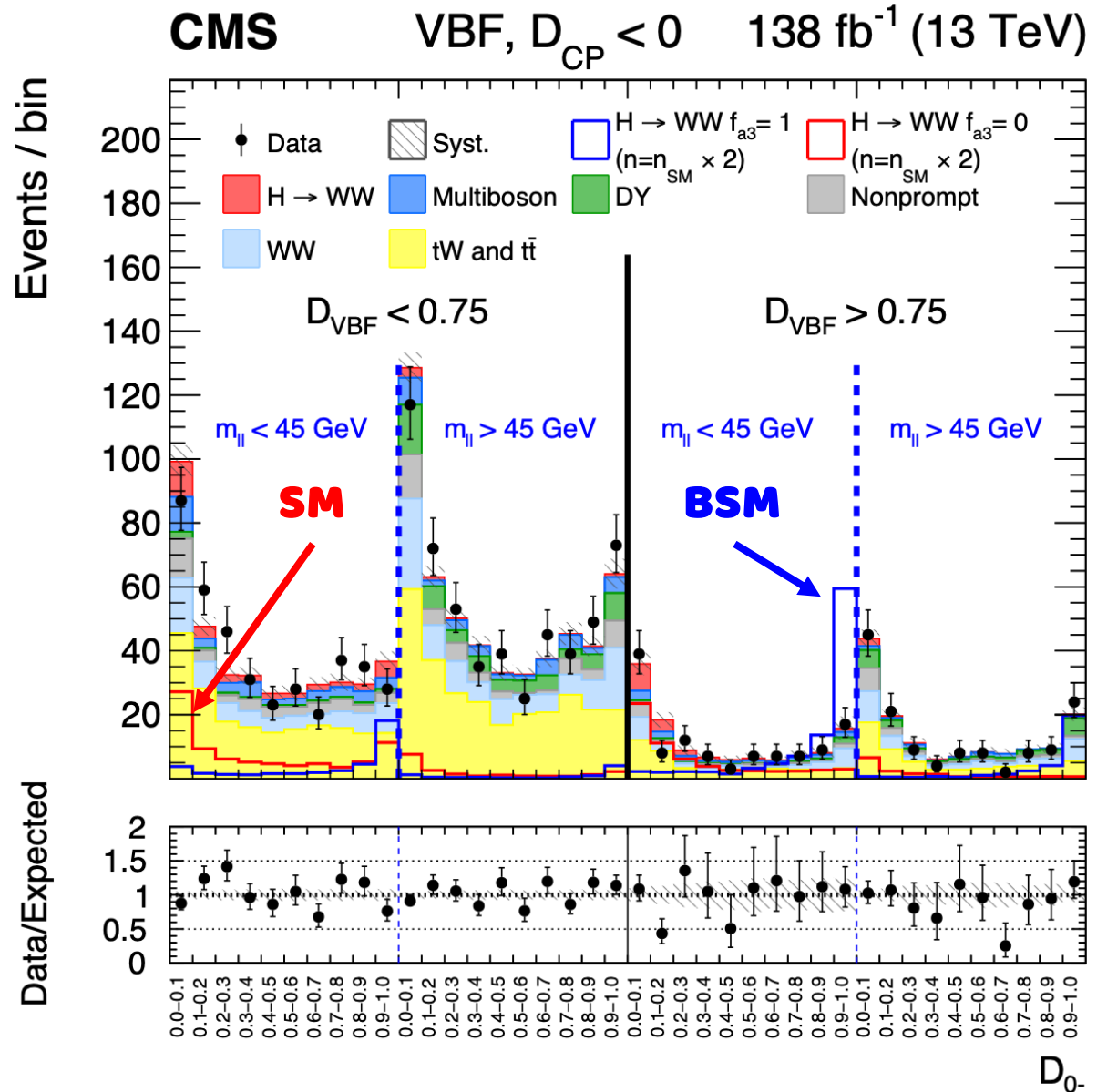
Pure BSM contribution (D_{0^-})

SM-BSM interferences (D_{CP})

Sensitive to decay vertex:

$m_{\ell\ell}$

Fit to multidimensional KD



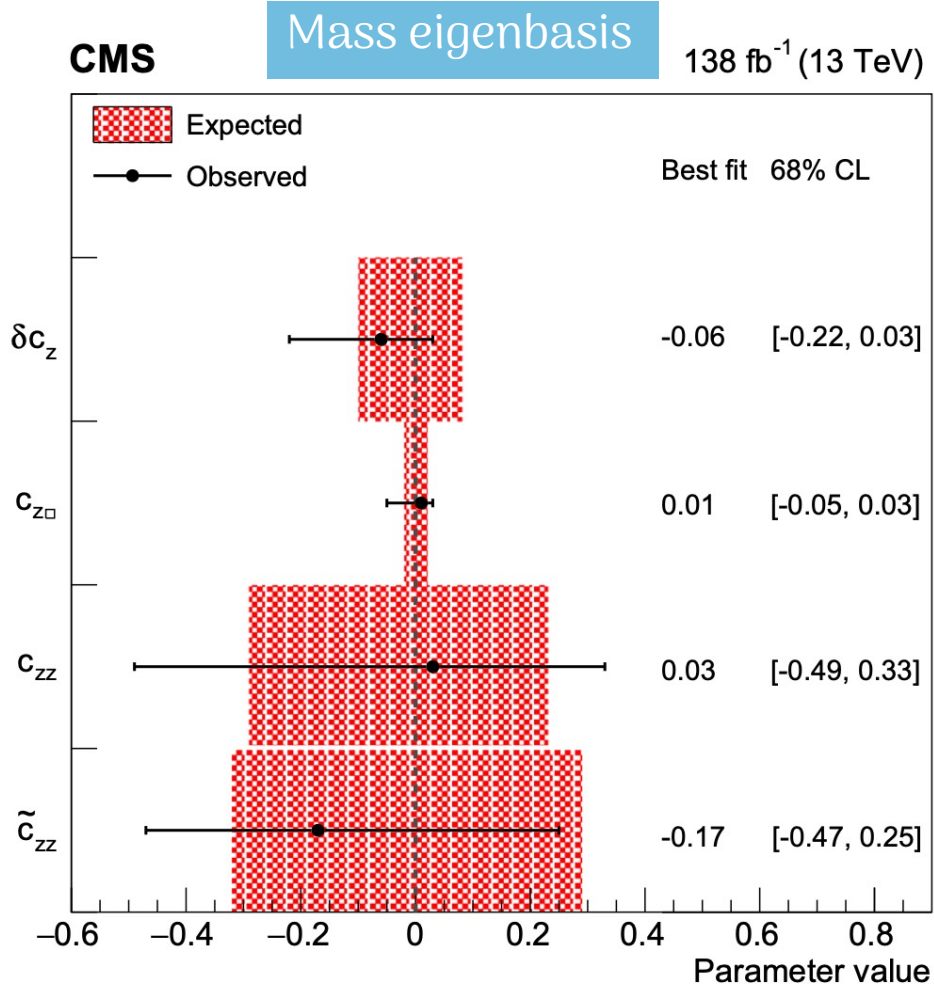
SMEFT Higgs basis

Useful for analyses combination

Linear+Quadratic

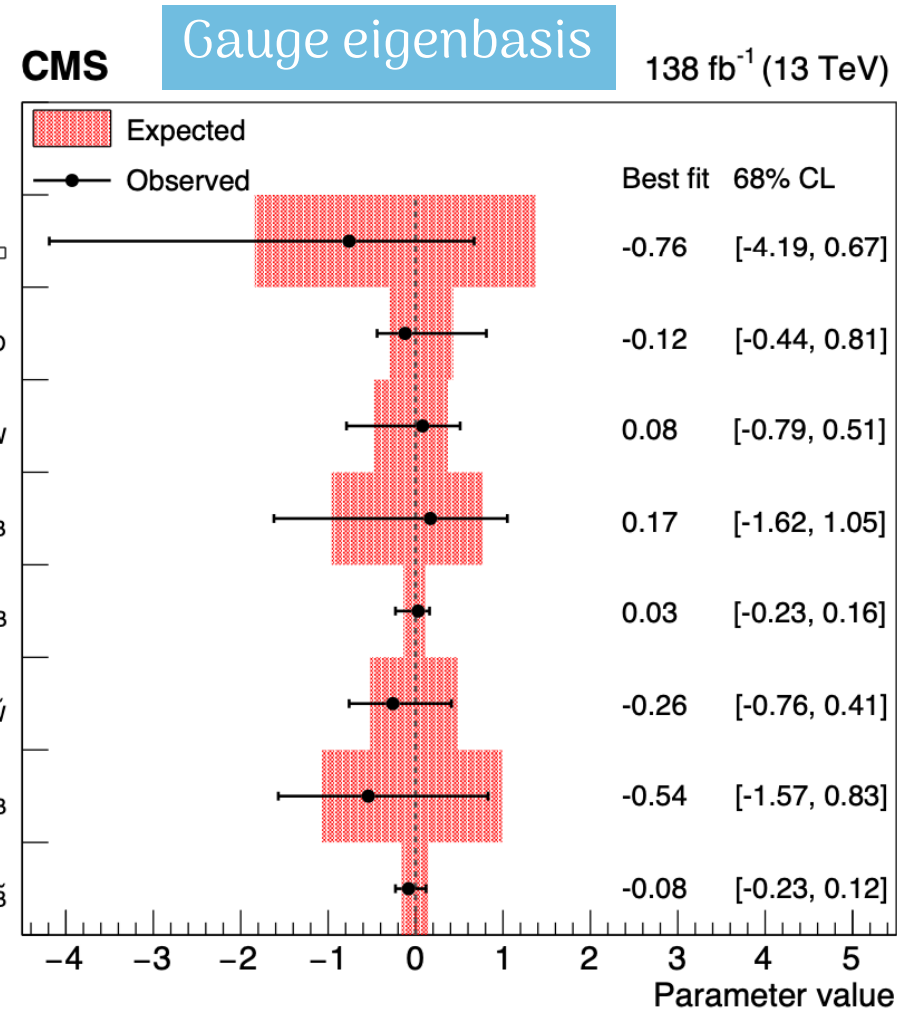
SMEFT Warsaw basis

Useful for the theoretician community

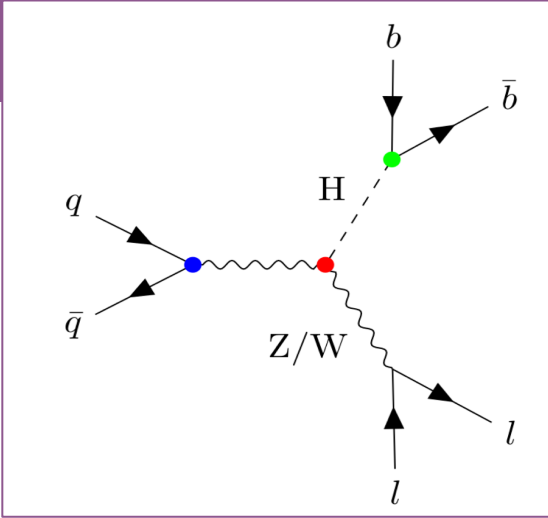


Surpassing results of [Run 1 analysis](#) in precision and coverage.

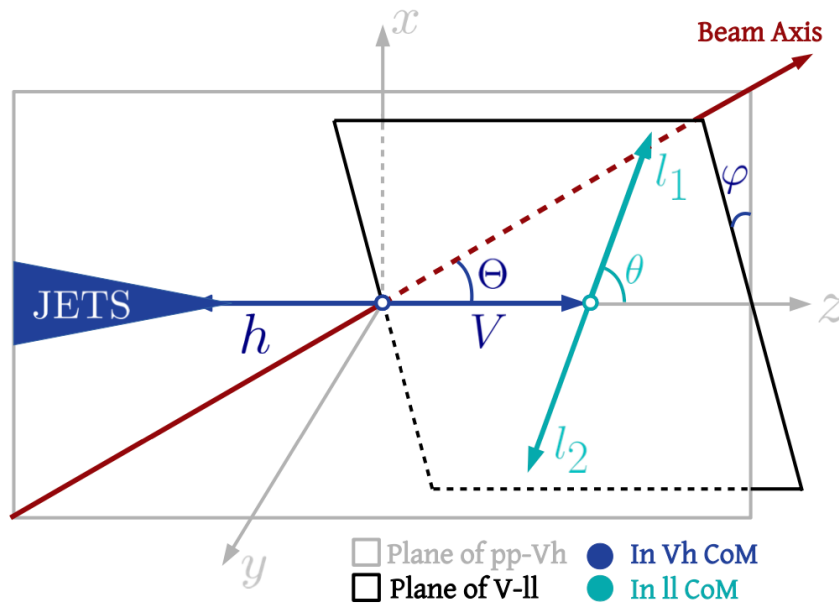
Wilson Coefficients
(3 independent fits to the data)



Results in terms of cross section fraction contribution available.



**Also based on likelihood ratios
but with reconstructed objects
after detector smearing**



Decay Channels:

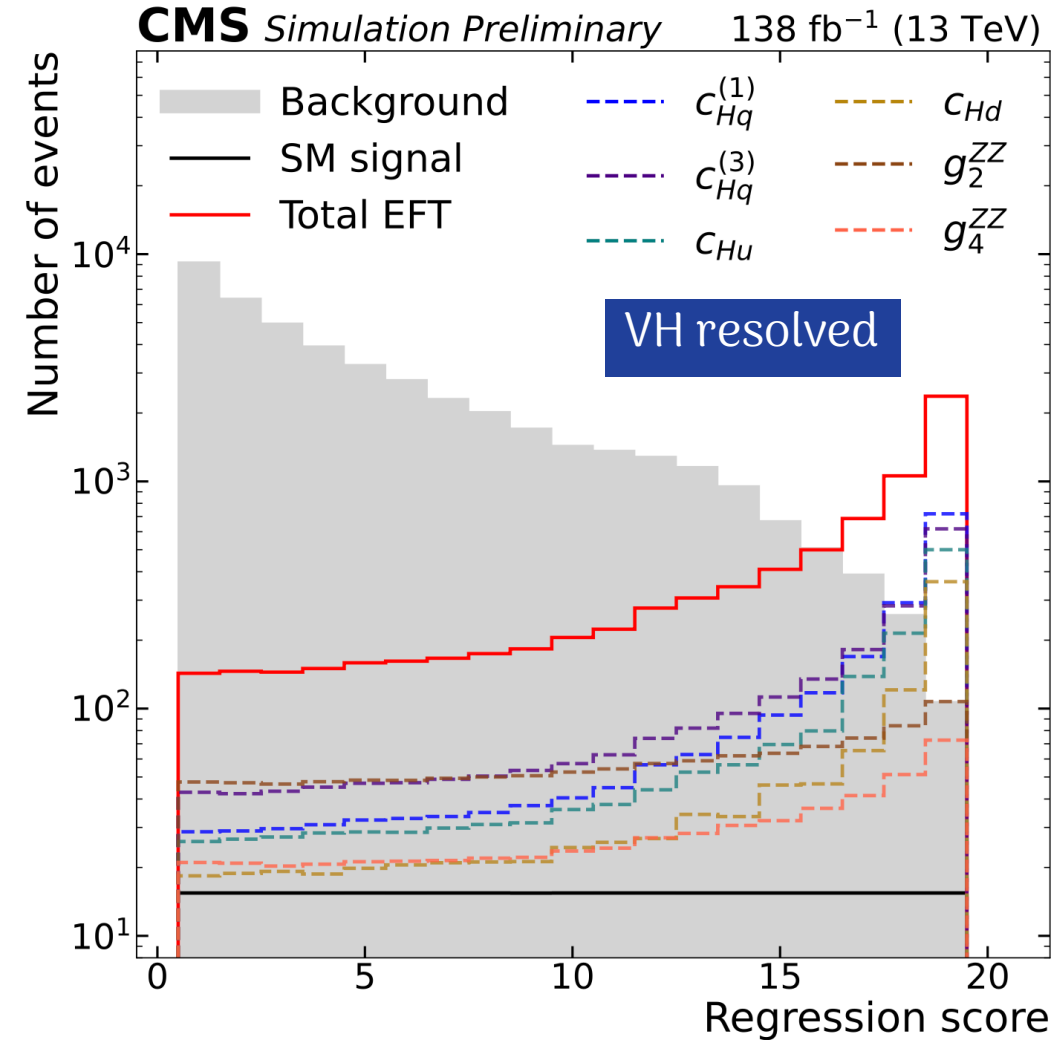
- 0 leptons: $Z \rightarrow \nu\nu$
- 1 lepton: $W \rightarrow \ell\nu$
- 2 leptons: $Z \rightarrow \ell\ell$

Fit to observables:

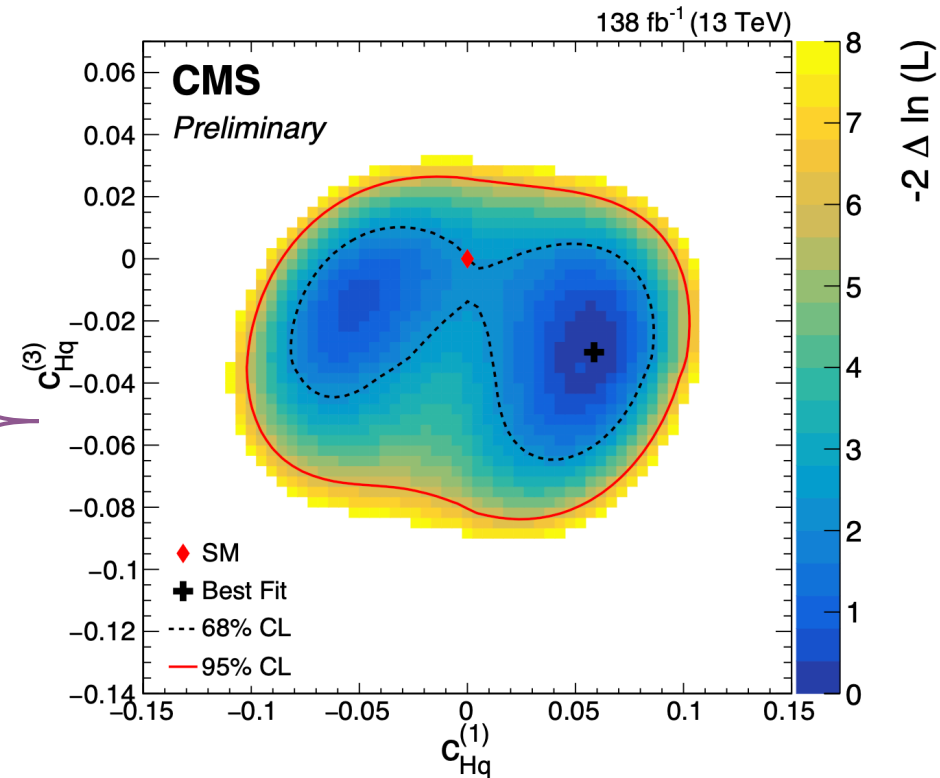
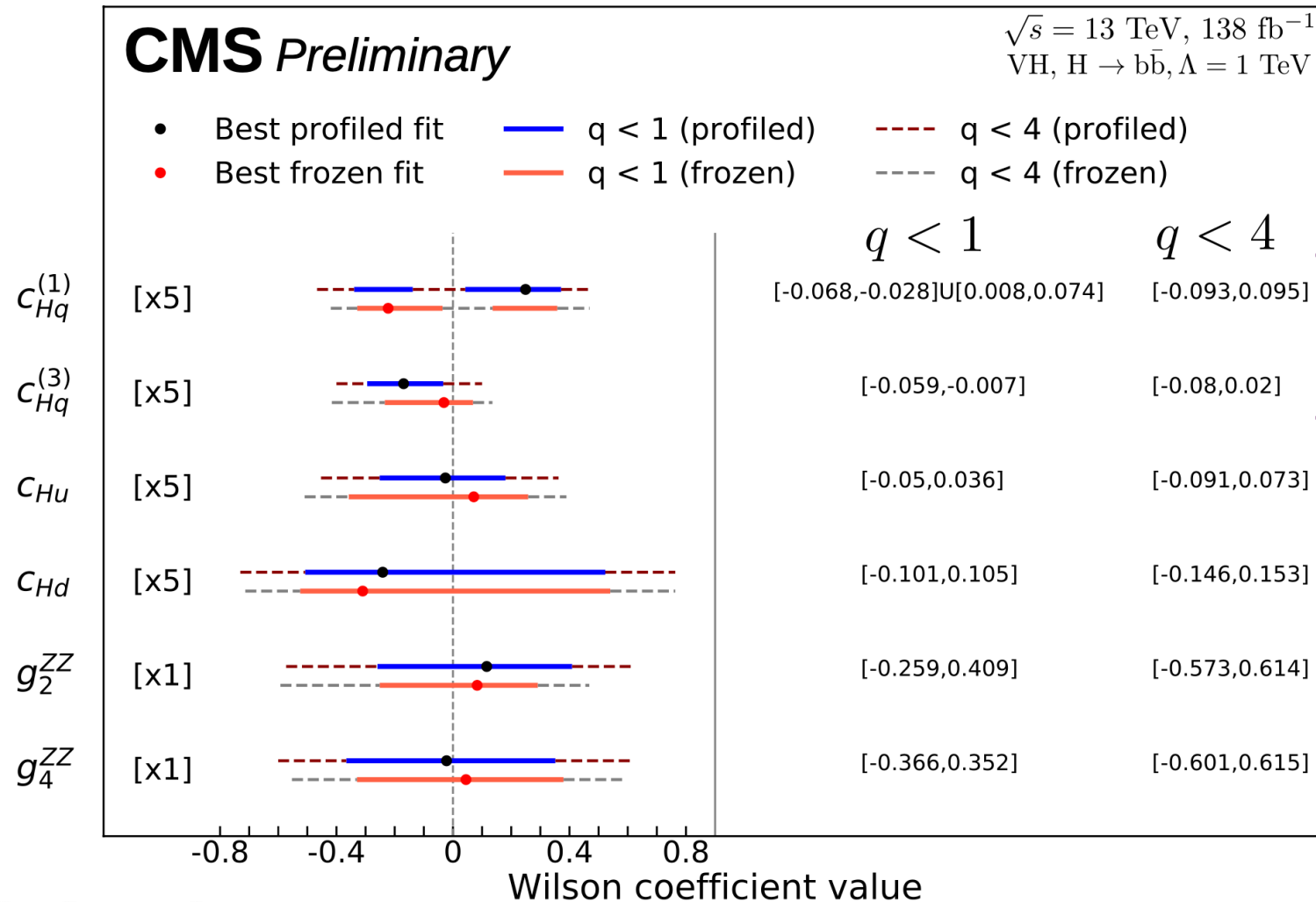
Boosted information Trees (BIT)

Observables optimized for the EFT effects

[Data/MC plots for reference](#)



Constraints on Wilson Coefficients



Results are consistent with the SM expectation

$$g_2^{ZZ} \propto s_w^2 C_{HB} + c_w^2 C_{HW} + s_w c_w C_{HWB}$$

$$g_4^{ZZ} \propto s_w^2 C_{H\bar{B}} + c_w^2 C_{H\bar{W}} + s_w c_w C_{H\bar{W}B}$$

EFT in $HZ\gamma$ and $H\gamma\gamma$

CMS-PAS-HIG-23-011

Targeting the production vertex involving the Higgs and an associated photon, these AC can impact the production rate

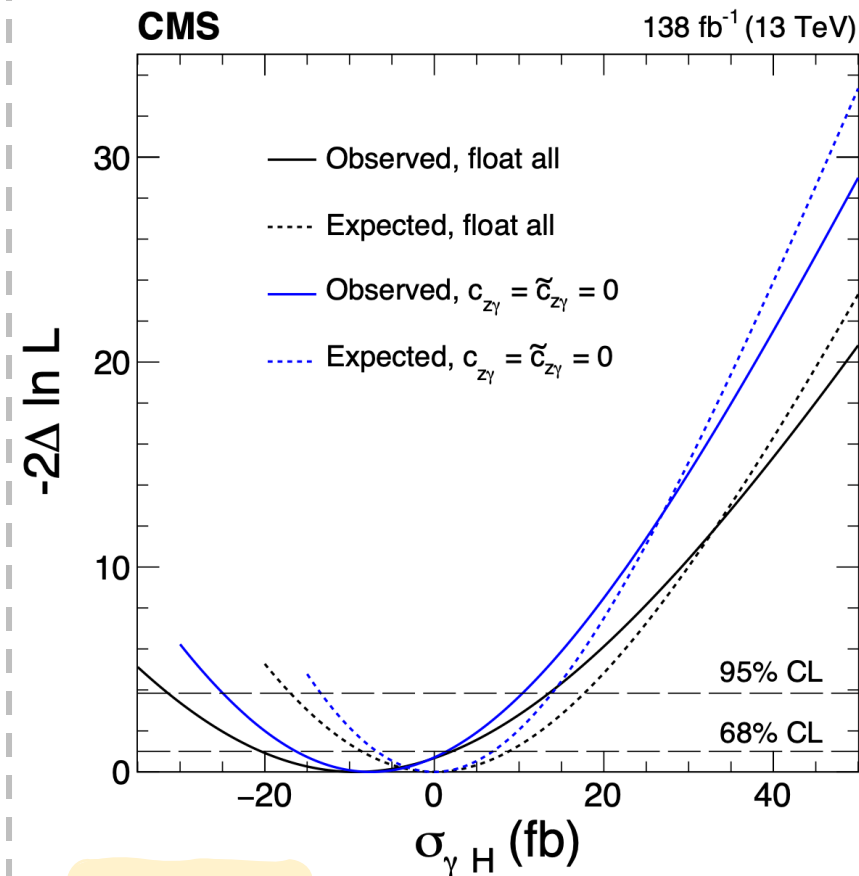
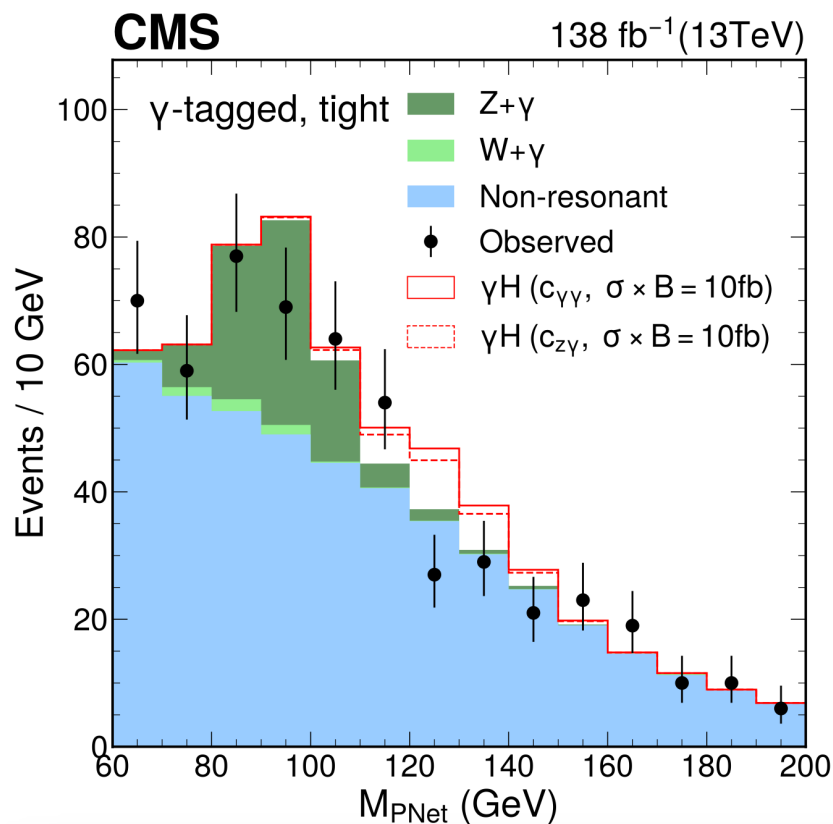
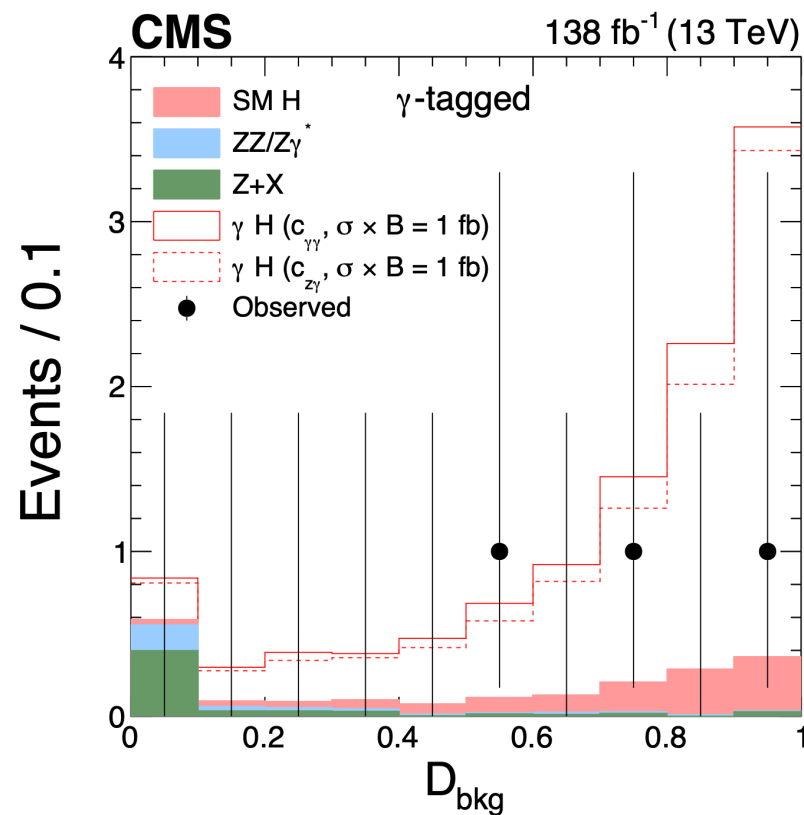
$H \rightarrow ZZ \rightarrow 4\ell$

$H \rightarrow b\bar{b}$

Cross-section measurement from the combination of channels

MELA-based discriminants

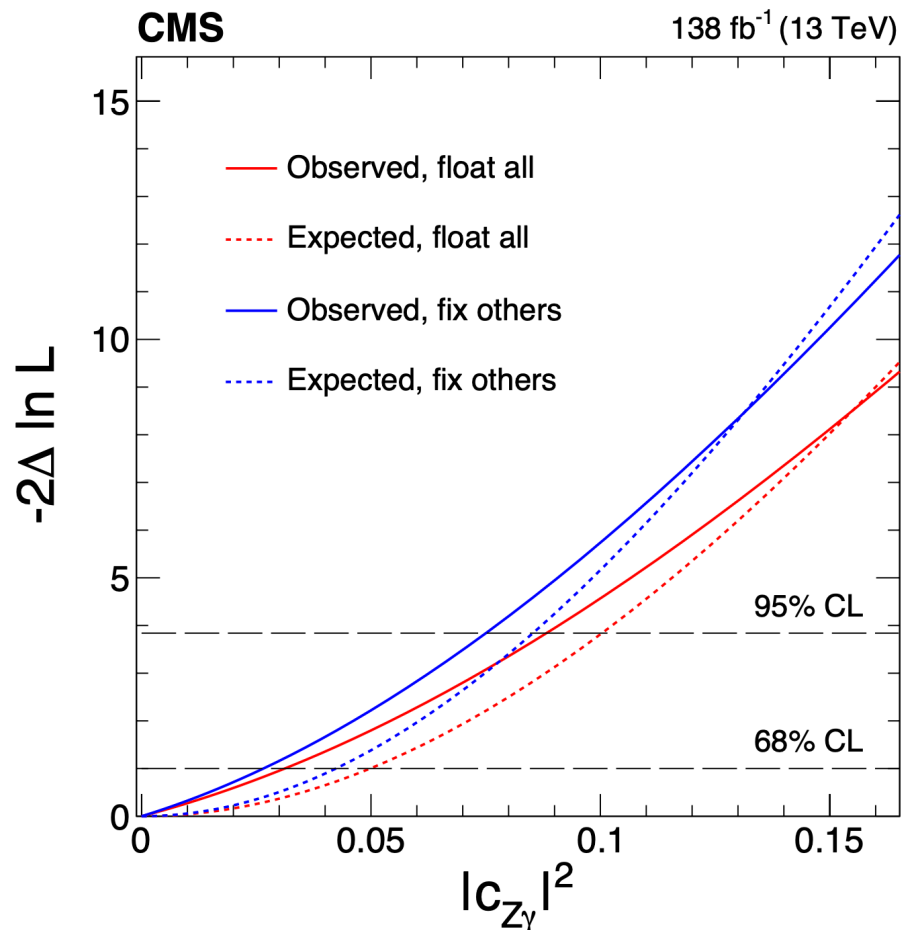
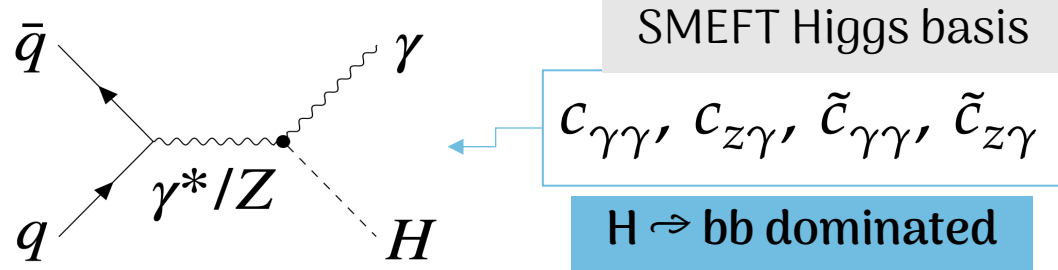
Mass of Higgs candidate



Fitted observables

Result

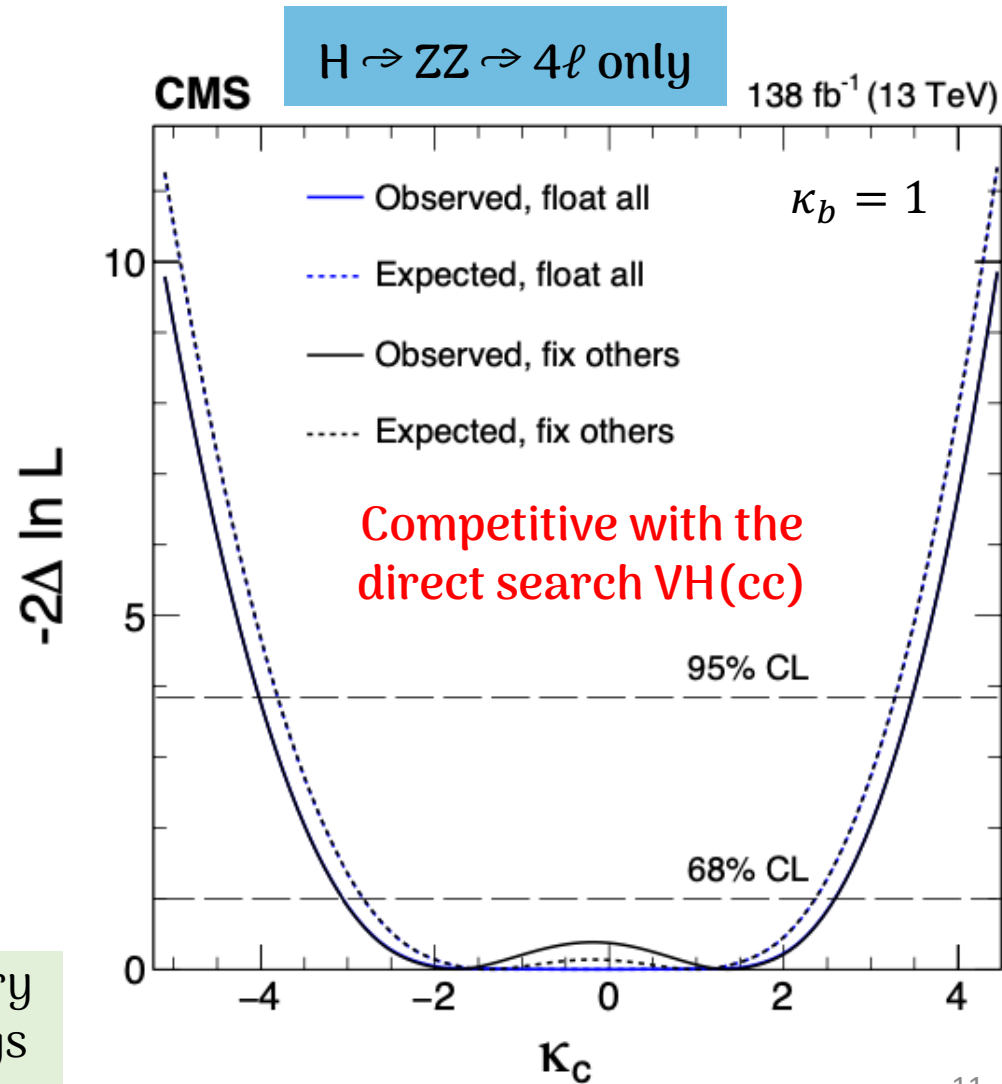
HVV couplings scans



Supplementary
 result on Higgs
 Width Γ_{BSM}^H

Yukawa couplings scans

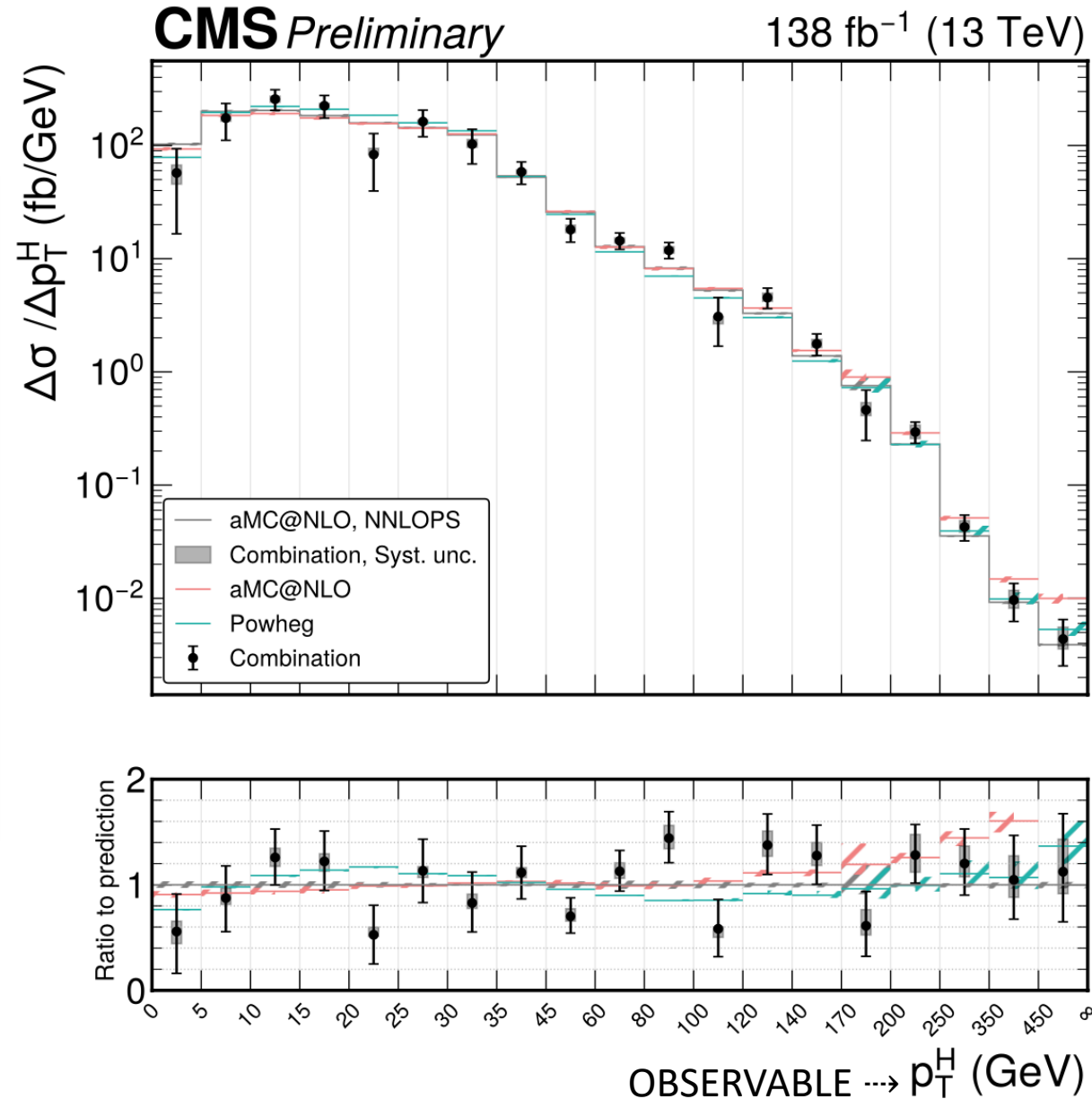
Hff vertex parametrization $\kappa_u, \kappa_d, \kappa_s,$ and κ_c



Combination and EFT interpretation of Higgs differential fiducial measurements

[CMS-PAS-HIG-23-013](#)

$H \rightarrow \gamma\gamma$ JHEP 07 (2023) 091
$H \rightarrow ZZ \rightarrow 4\ell$ JHEP 08 (2023) 040
$H \rightarrow WW \rightarrow e\mu\nu\nu$ JHEP 03 (2021) 003
$H \rightarrow \tau\tau$ Phys. Rev. Lett. 128 (2022) 081805
$H \rightarrow \tau\tau$ (boosted) Phys. Lett. B 857 (2024) 138964



Analysis strategy:

Differential distributions are sensitive to Higgs couplings through distortions in the predicted SM cross-section spectra.

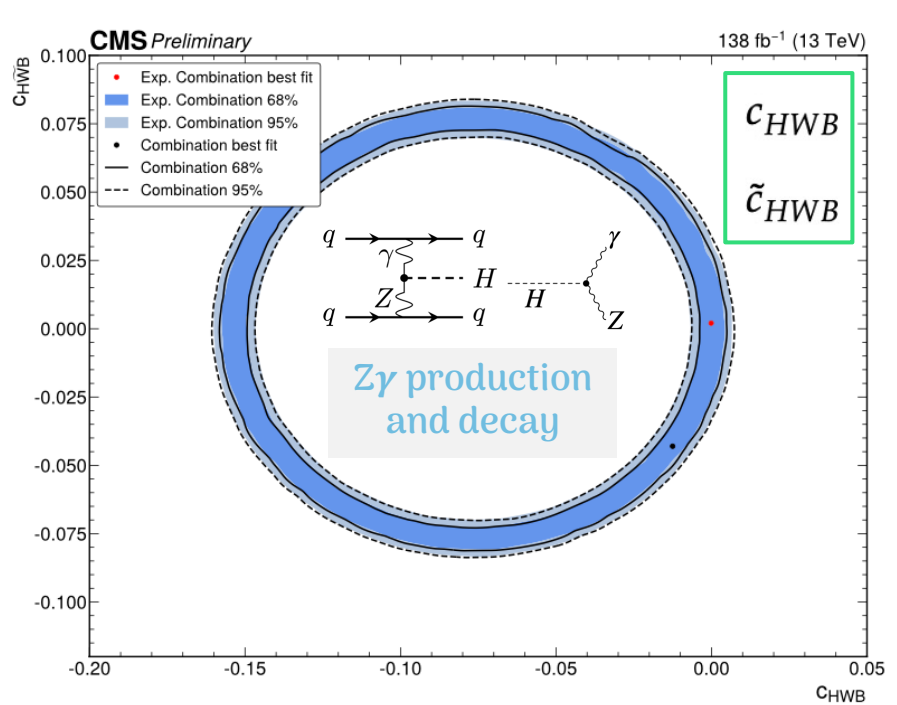
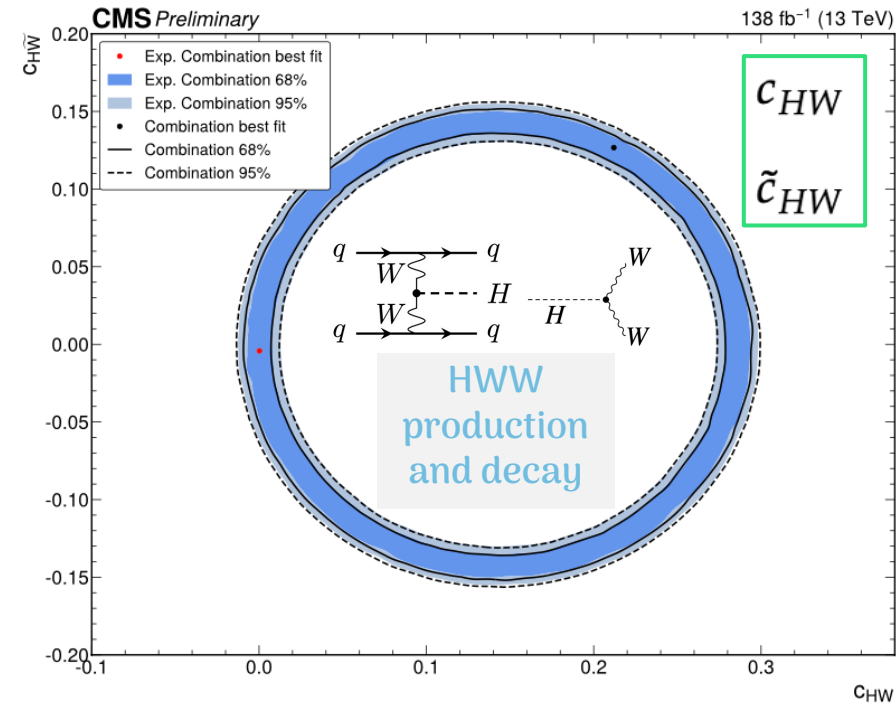
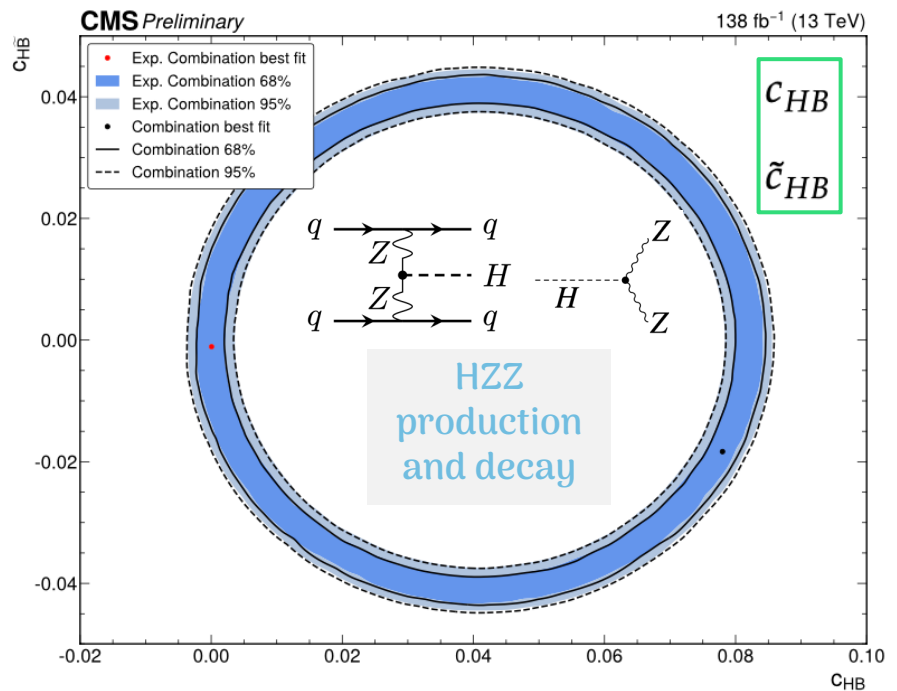
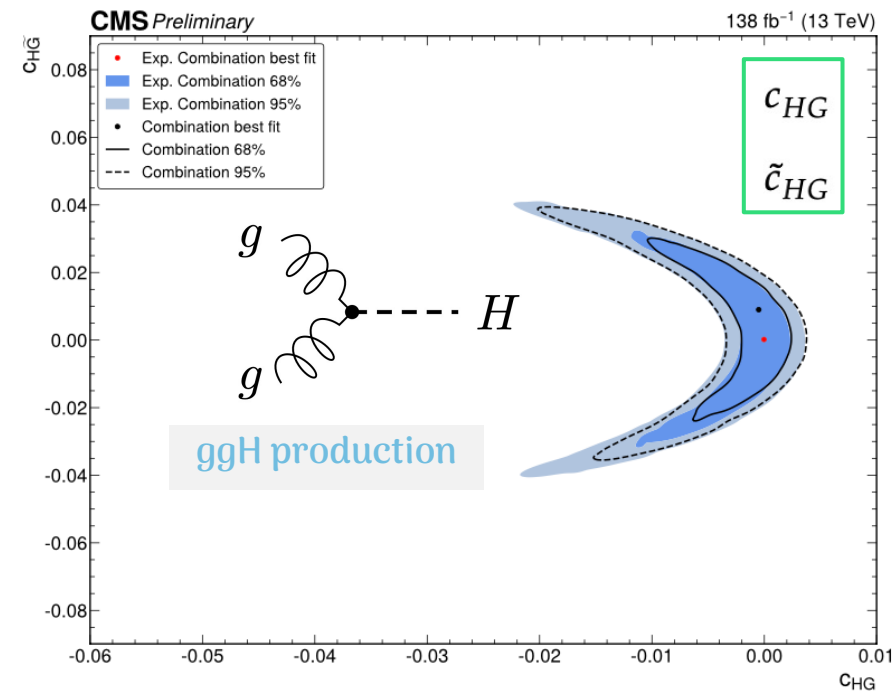
Used parametrizations:

κ -framework and **SMEFT**

p_T^H 2D scans of Wilson coefficients

Fit **pairs** of CP-even and CP-odd Wilson coefficients to assess their impact on Higgs production and decay, with all other coefficients set to their SM values of zero.

But there are more...!



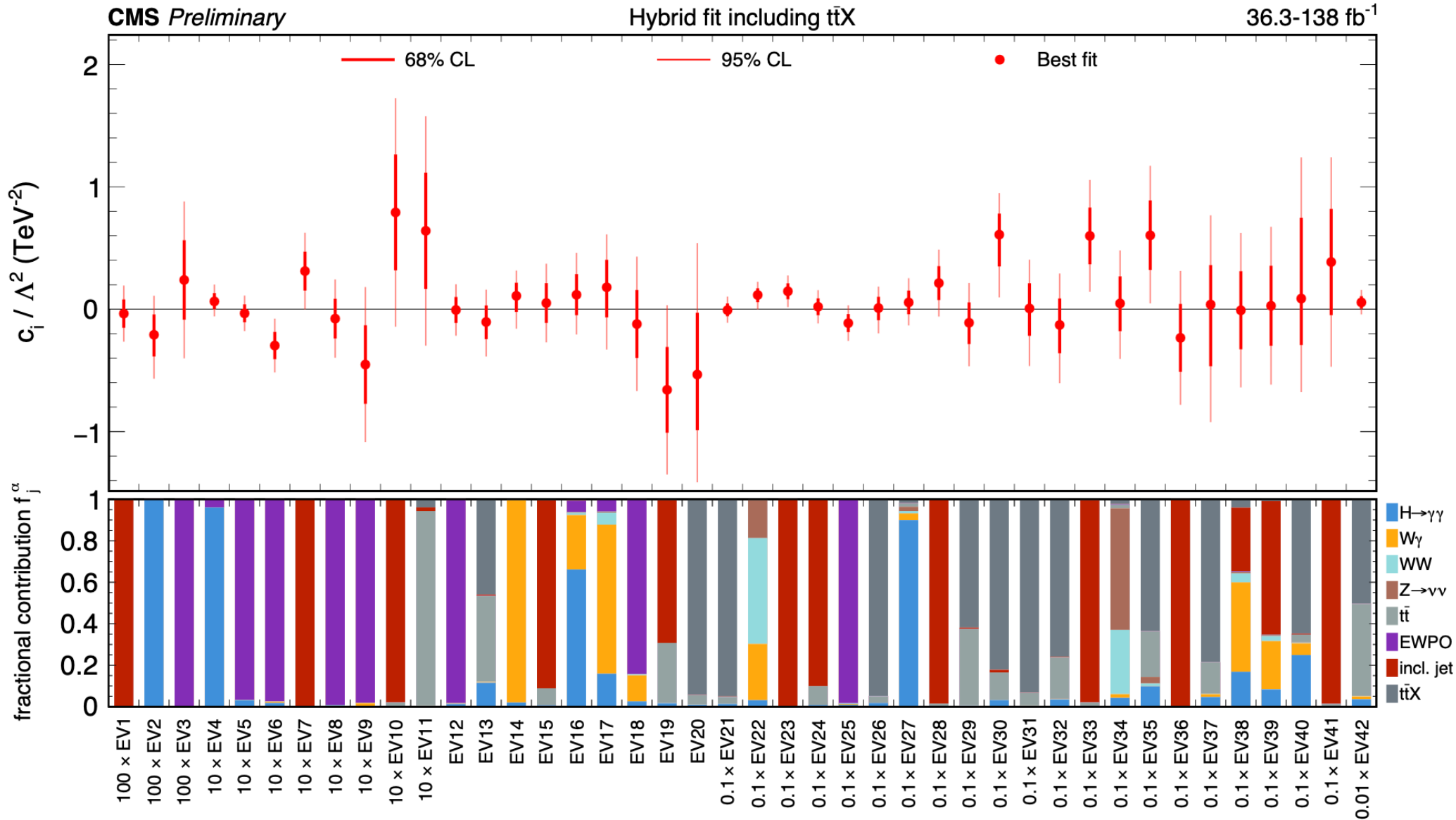
Combined EFT interpretation of SM measurements

First combination from an experiment including top, Higgs, vector boson and jet measurements in an EFT interpretation!

Analysis	Type of measurement	Observables used	Experimental likelihood
$H \rightarrow \gamma\gamma$	Diff. cross sections	STXS bins [40]	✓
$W\gamma$	Fid. diff. cross sections	$p_T^\gamma \times \phi_f $	✓
WW	Fid. diff. cross sections	$m_{\ell\ell}$	✓
$Z \rightarrow \nu\nu$	Fid. diff. cross sections	p_T^Z	✓
$t\bar{t}$	Fid. diff. cross sections	$M_{t\bar{t}}$	×
EWPO	Pseudo-observables	$\Gamma_Z, \sigma_{\text{had}}^0, R_\ell, R_c, R_b, A_{FB}^{0,\ell}, A_{FB}^{0,c}, A_{FB}^{0,b}$	×
Inclusive jets	Fid. diff. cross sections	$p_T^{\text{jet}} \times y^{\text{jet}} $	×
$t\bar{t}X$	Direct EFT	Yields in regions of interest	✓

✓ LEP and SLC electroweak precision measurements included.

Flash of the EV fit



42 directions are constrained simultaneously... The most so far!

Supplementary result on 95% CL lower limits on the scales Λ of NP $\sim \text{TeV}$

Conclusions

- EFT serves as a connection to the fundamental nature of interactions, bridging different energy scales.
- 5 indirect searches of BSM effects in the context of SMEFT have been presented across:
 - 3 individual channels, refining our understanding of Higgs couplings to particles and the EWSB mechanism.
 - Two combined EFT interpretation analyses on the Higgs and SM demonstrate that global EFT data analyses are crucial.
- EFT Run 2 analyses are statistically limited but show promise for future Higgs physics in Run 3 and beyond.
- For now, everything is consistent with the SM within uncertainties.
- Precision is key — accurate approximations are essential to staying safe and sound!





BACK UP SLIDES

EFT $H \rightarrow WW \rightarrow e\mu\nu\nu$ analysis

Targeting HVV anomalous couplings in production and decay vertexes

Matrix Element Likelihood Approach (MELA)

Analysis strategy:

MELA-based kinematic discriminants (KD)

Production channels:

ggH, VBF, VH, and boosted VH

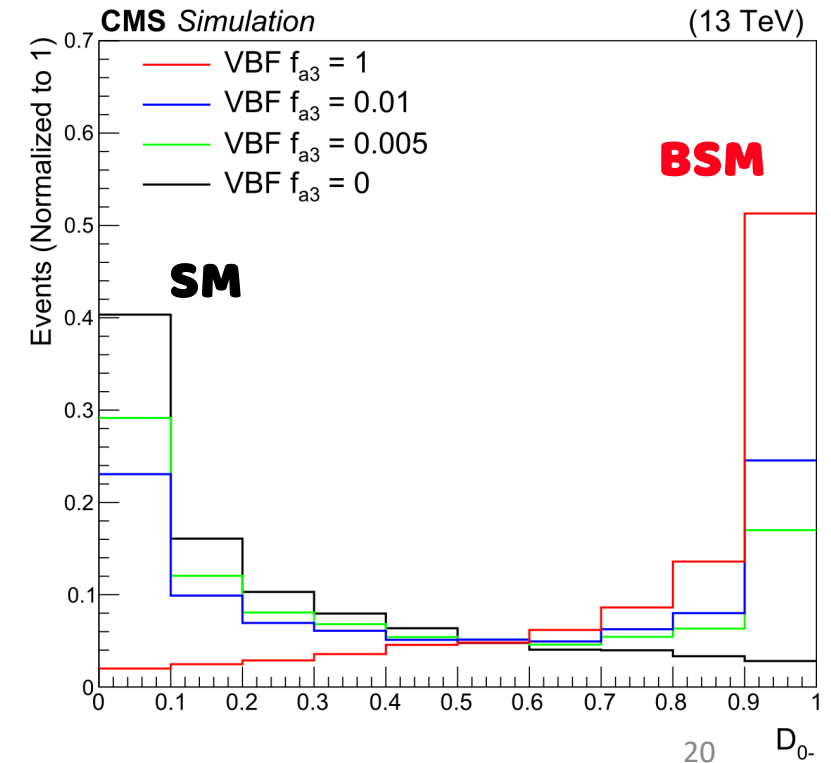
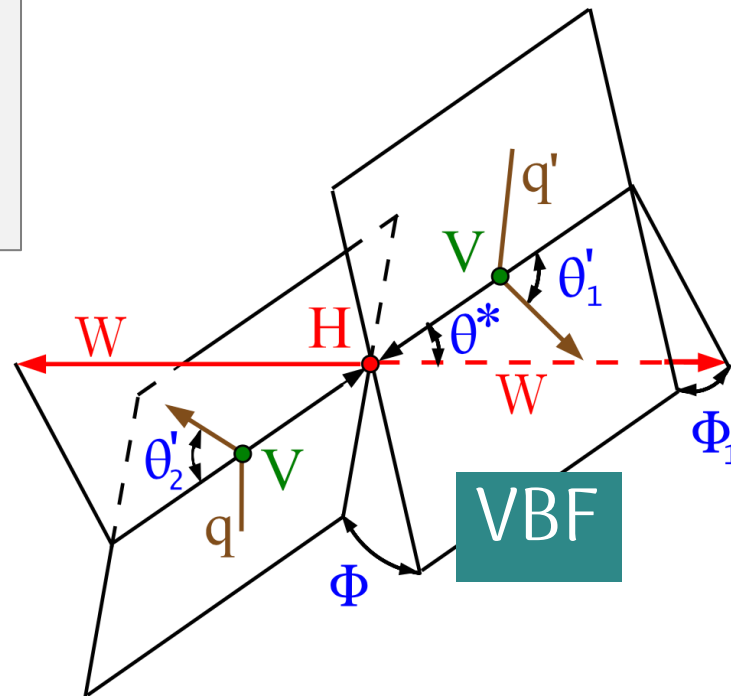
Used approaches:

AC and SMEFT

Reconstructed event
Theoretical hypothesis

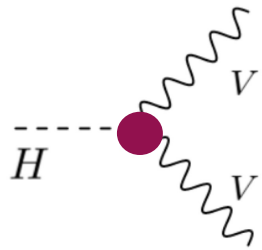


Probability that the event matches the hypothesis



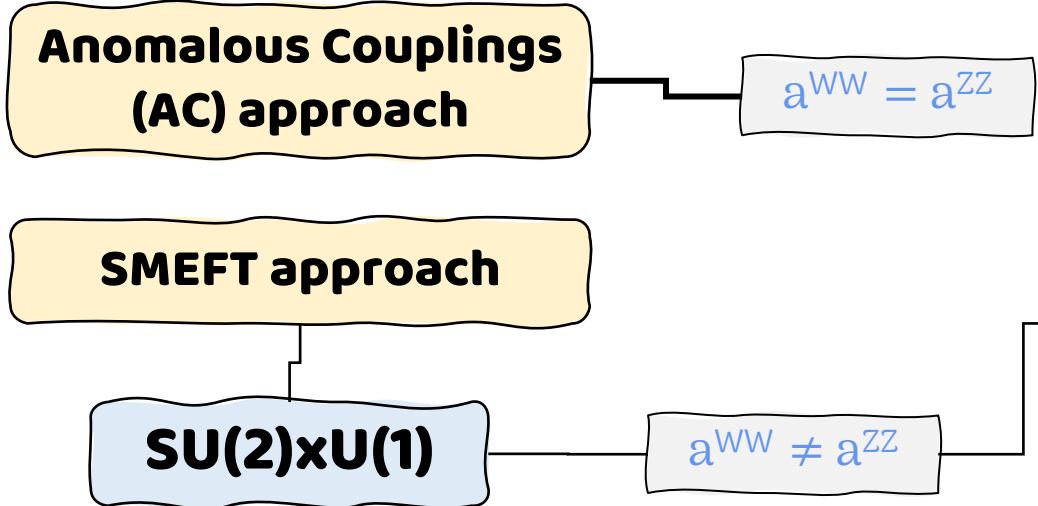
HVV vertex parametrization

Scattering amplitude :



$$A(HV_1V_2) \sim \left[\overset{\text{SM}}{a_1^{\text{VV}}} + \frac{\kappa_1^{\text{VV}} q_{V1}^2 + \kappa_2^{\text{VV}} q_{V2}^2}{(\Lambda_1^{\text{VV}})^2} \right] m_{V1}^2 \epsilon_{V1}^* \epsilon_{V2}^* + \frac{1}{v} a_2^{\text{VV}} f_{\mu\nu}^{*(1)} f^{*(2),\mu\nu} + \frac{1}{v} a_3^{\text{VV}} f_{\mu\nu}^{*(1)} \tilde{f}^{*(2),\mu\nu}$$

Higher-order SM loop or BSM contributions (anomalous couplings)



Simultaneously studied: a_1, a_2, a_3 (CP-odd) and $a_{\Lambda 1}$

Results can be given in terms of:

1. Cross-section fraction f_{ai} (+ μ on signal model):

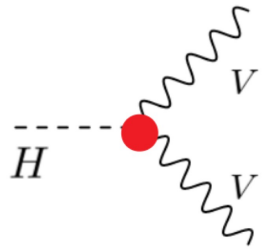
$$f_{ai} = \frac{|a_i|^2 \sigma_i}{\sum_j |a_j|^2 \sigma_j} \text{sign} \left(\frac{a_i}{a_1} \right)$$

2. SMEFT Mass eigen (Higgs) basis
3. SMEFT Gauge eigen (Warsaw) basis



HVV vertex parametrization

Scattering amplitude :



$$A(HV_1V_2) \sim \left[a_1^{\text{VV}} + \frac{\kappa_1^{\text{VV}} q_{V1}^2 + \kappa_2^{\text{VV}} q_{V2}^2}{(\Lambda_1^{\text{VV}})^2} \right] m_{V1}^2 \epsilon_{V1}^* \epsilon_{V2}^* + \frac{1}{v} a_2^{\text{VV}} f_{\mu\nu}^{*(1)} f^{*(2),\mu\nu} + \frac{1}{v} a_3^{\text{VV}} f_{\mu\nu}^{*(1)} \tilde{f}^{*(2),\mu\nu}$$

Higher-order SM loop or BSM contributions (anomalous couplings)

SU(2)xU(1)

Relationships between a^{WW} and a^{ZZ}

$$\frac{\kappa_1^{\text{WW}}}{(\Lambda_1^{\text{WW}})^2} = \frac{1}{c_w^2 - s_w^2} \left(\frac{\kappa_1^{\text{ZZ}}}{(\Lambda_1^{\text{ZZ}})^2} - 2s_w^2 \frac{a_2^{\text{ZZ}}}{M_Z^2} \right)$$

$$\frac{\kappa_2^{\text{Z}\gamma}}{(\Lambda_1^{\text{Z}\gamma})^2} = \frac{2s_w c_w}{c_w^2 - s_w^2} \left(\frac{\kappa_1^{\text{ZZ}}}{(\Lambda_1^{\text{ZZ}})^2} - \frac{a_2^{\text{ZZ}}}{M_Z^2} \right)$$

$$a_1^{\text{WW}} = a_1^{\text{ZZ}}$$

$$a_2^{\text{WW}} = c_w^2 a_2^{\text{ZZ}}$$

$$a_3^{\text{WW}} = c_w^2 a_3^{\text{ZZ}}$$

SMEFT approach

Simultaneously studied: a_1, a_2, a_3 (CP-odd) and $a_{\Lambda 1}$

Results can be given in terms of:

1. Cross-section fraction f_{ai} (+ μ on signal model):

$$f_{ai} = \frac{|a_i|^2 \sigma_i}{\sum_j |a_j|^2 \sigma_j} \text{sign} \left(\frac{a_i}{a_1} \right)$$

2. SMEFT Mass eigen (Higgs) basis
3. SMEFT Gauge eigen (Warsaw) basis



$H \rightarrow WW \rightarrow e\mu\nu\nu$

CMS VBF, $D_{CP} < 0$ 138 fb⁻¹ (13 TeV)

MELA-based kinematic discriminants
(KD) sensitive to production vertex:

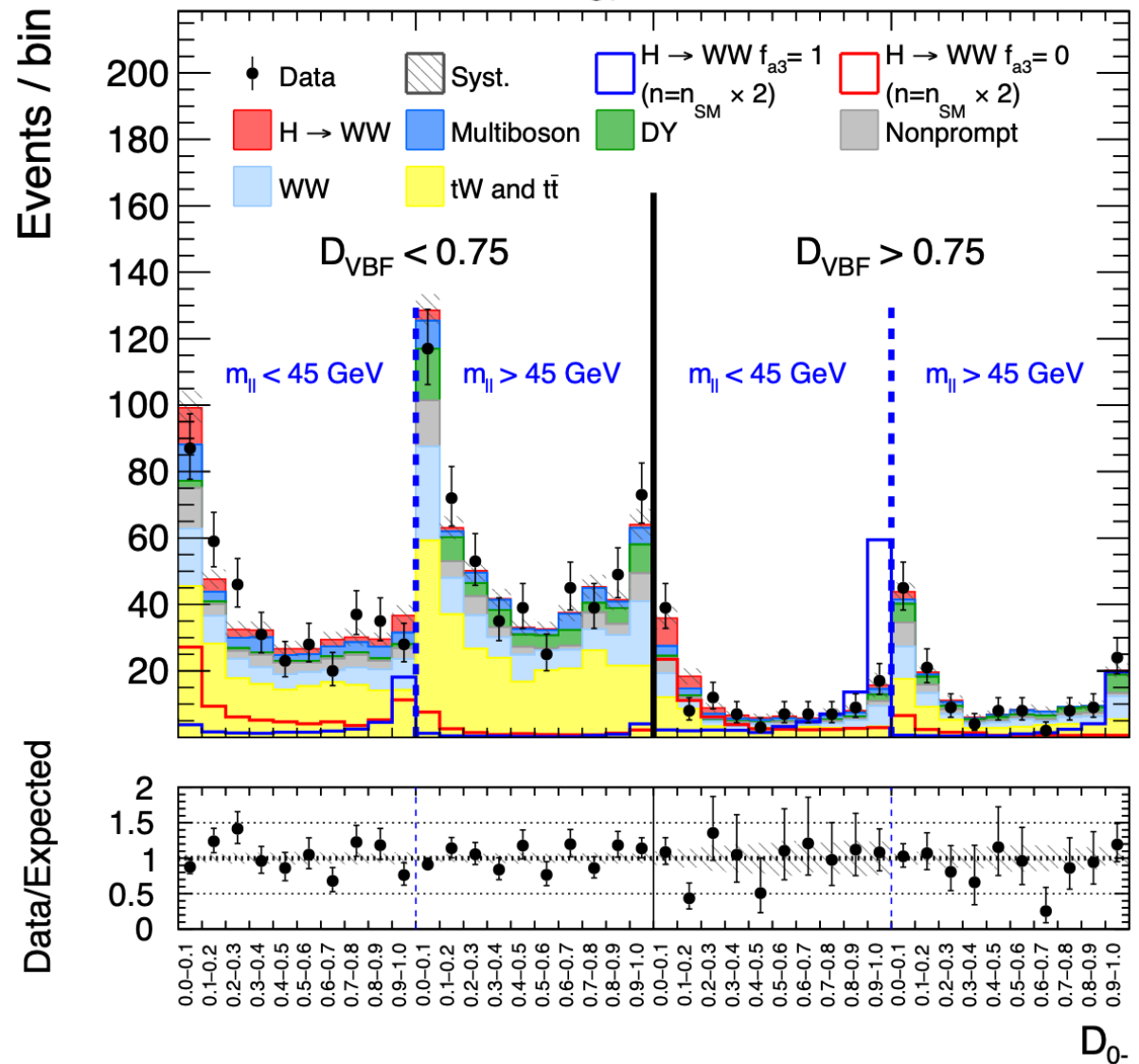
- Production mode (D_{VBF})
- Pure AC contribution (D_{0-})
- Interference AC contribution (D_{CP})

Sensitive to decay vertex:

$m_{\ell\ell}$

Fit to multidimensional KD

$[D_{VBF}, D_{0-}, m_{\ell\ell}]$
+
 D_{CP} categorization



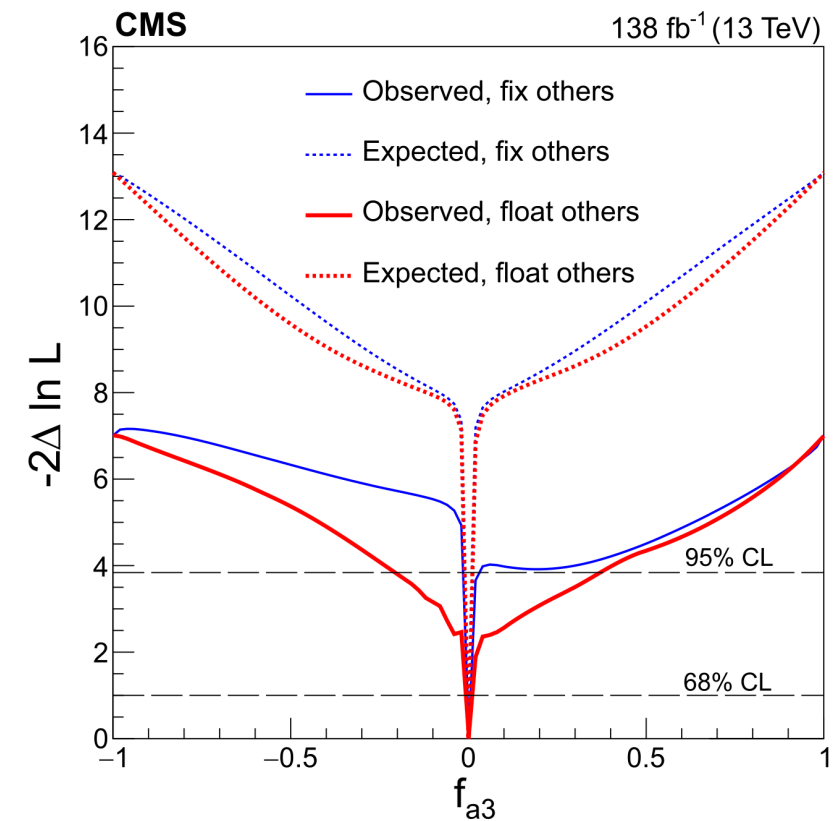
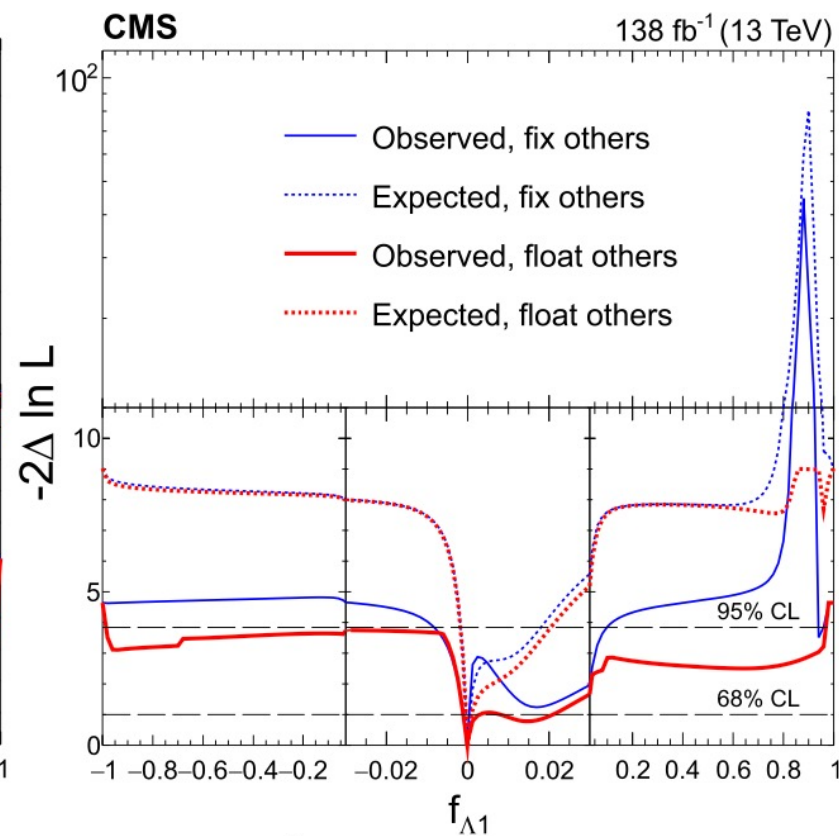
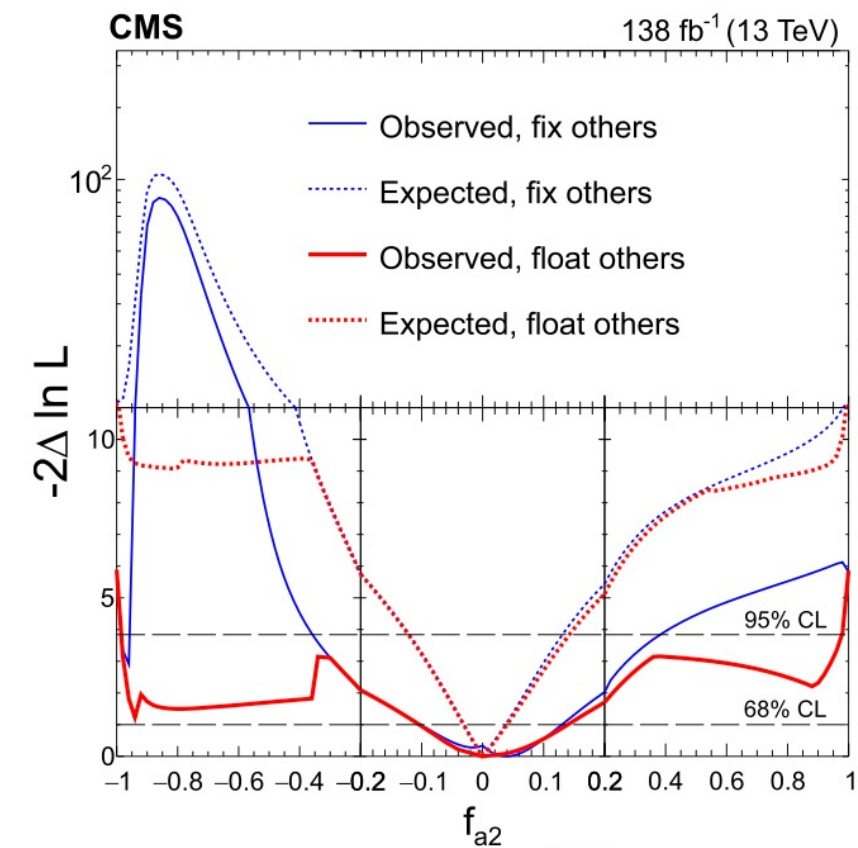
f_{ai} scans

SU(2)×U(1)

3 independent parameters

Results in terms of cross-section fraction

$$f_{ai} = \frac{|a_i|^2 \sigma_i}{\sum_j |a_j|^2 \sigma_j} \text{sign} \left(\frac{a_i}{a_1} \right)$$



Translation into SMEFT bases possible

AC SCANS

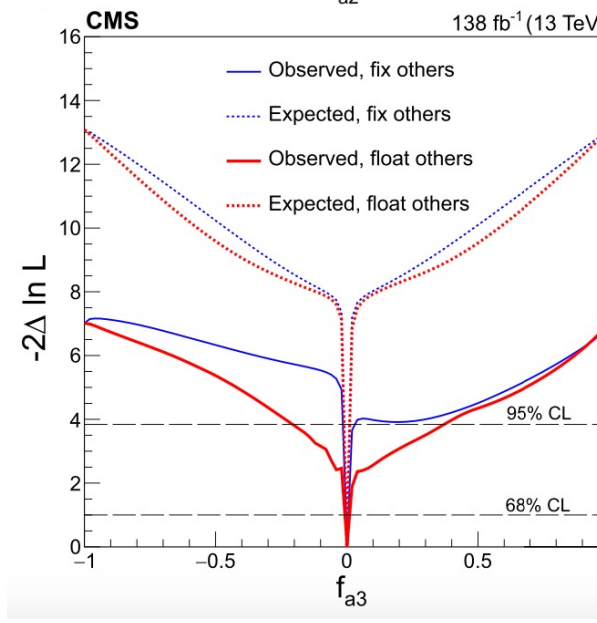
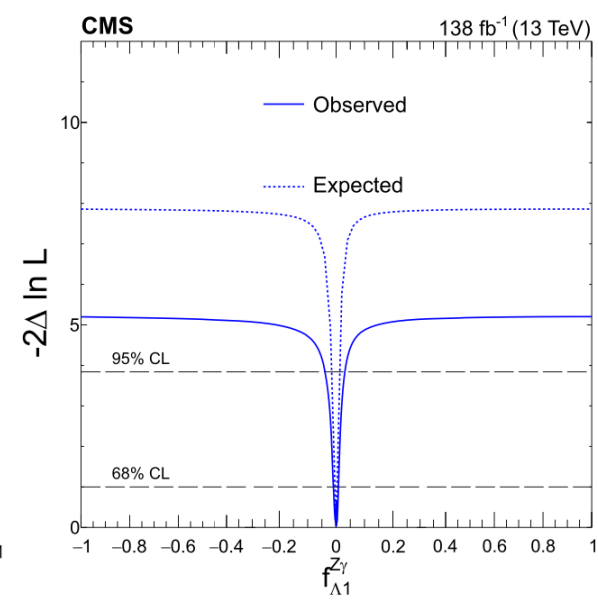
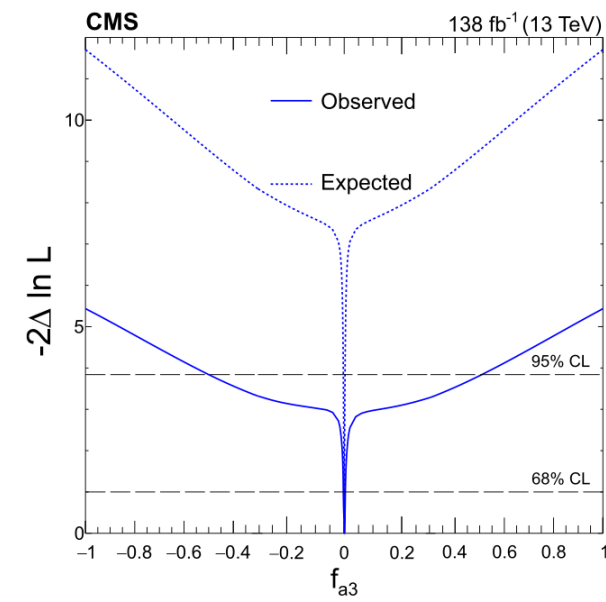
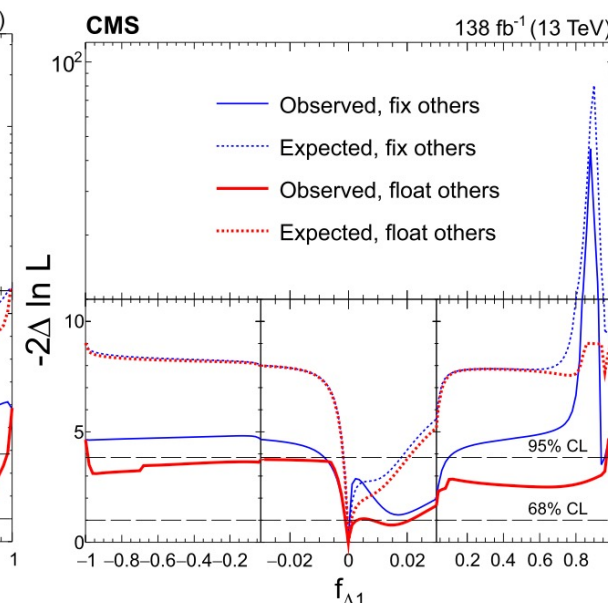
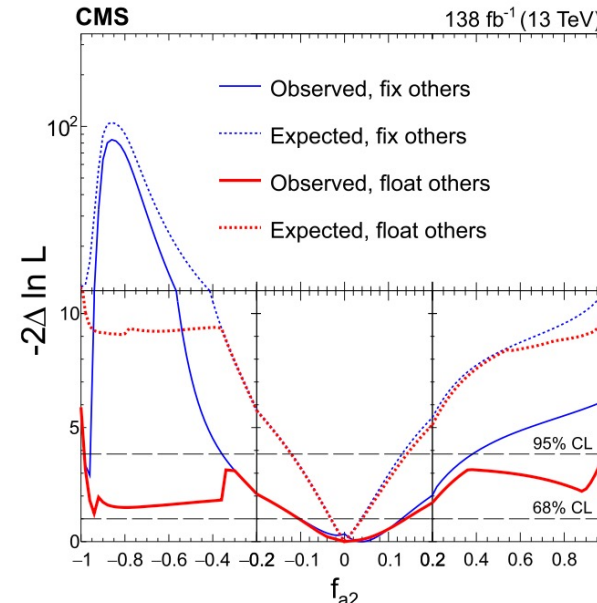
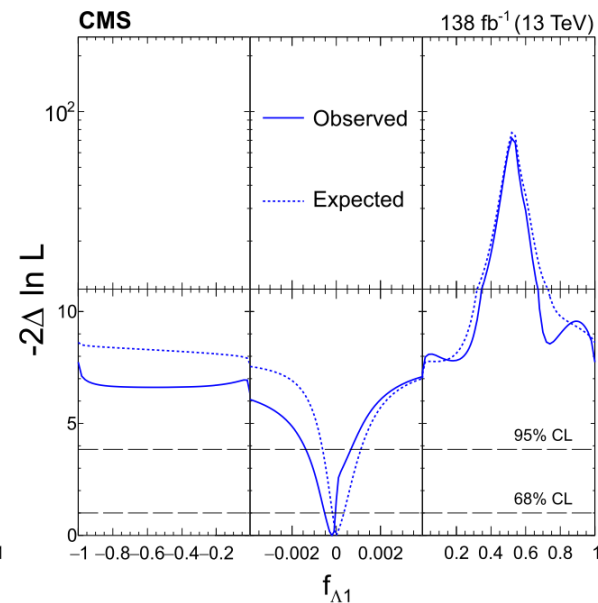
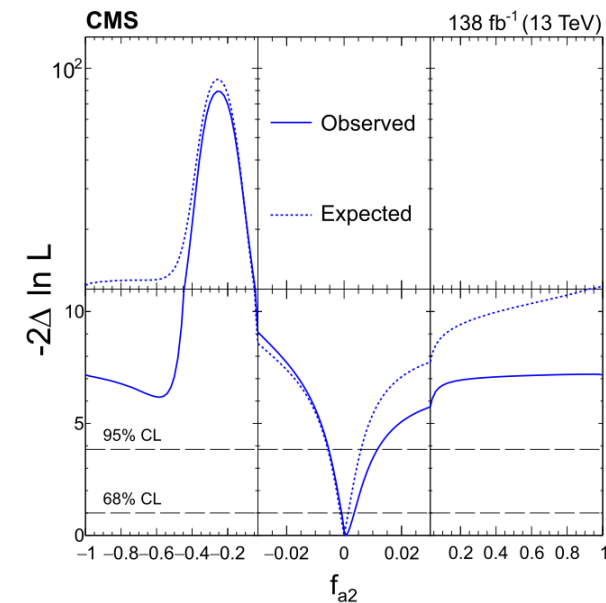
4 independent parameters

Results in terms of cross-section fraction f_{ai}

SMEFT SCANS

$SU(3) \times U(1)$

3 independent parameters



Translation into other SMEFT bases possible

SMEFT Higgs basis

Useful for analyses combination

$$\delta c_z = \frac{1}{2} a_1^{ZZ} - 1$$

$$c_{zz} = -\frac{2s_w^2 c_w^2}{e^2} a_2^{ZZ}$$

$$\tilde{c}_{zz} = -\frac{2s_w^2 c_w^2}{e^2} a_3^{ZZ}$$

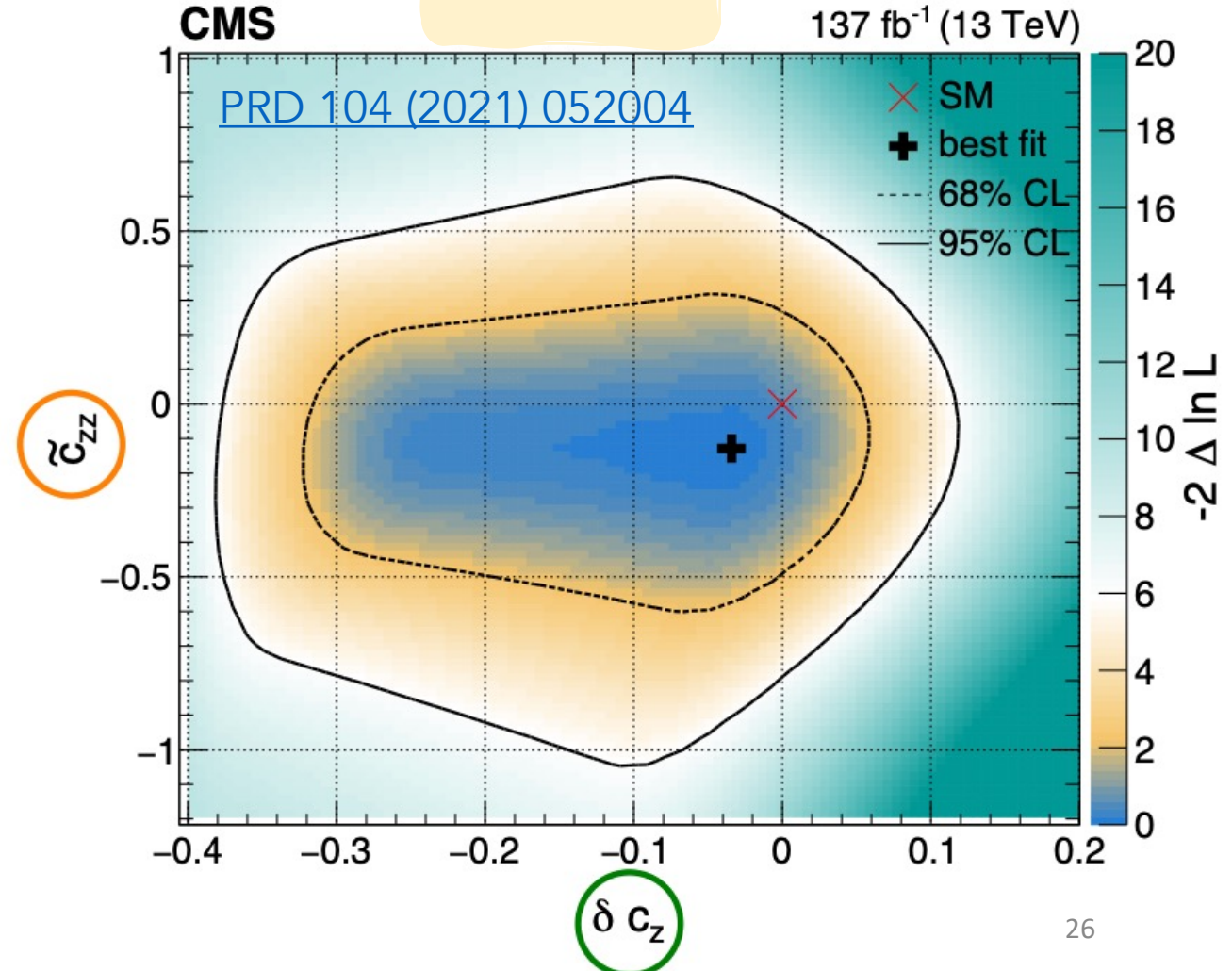
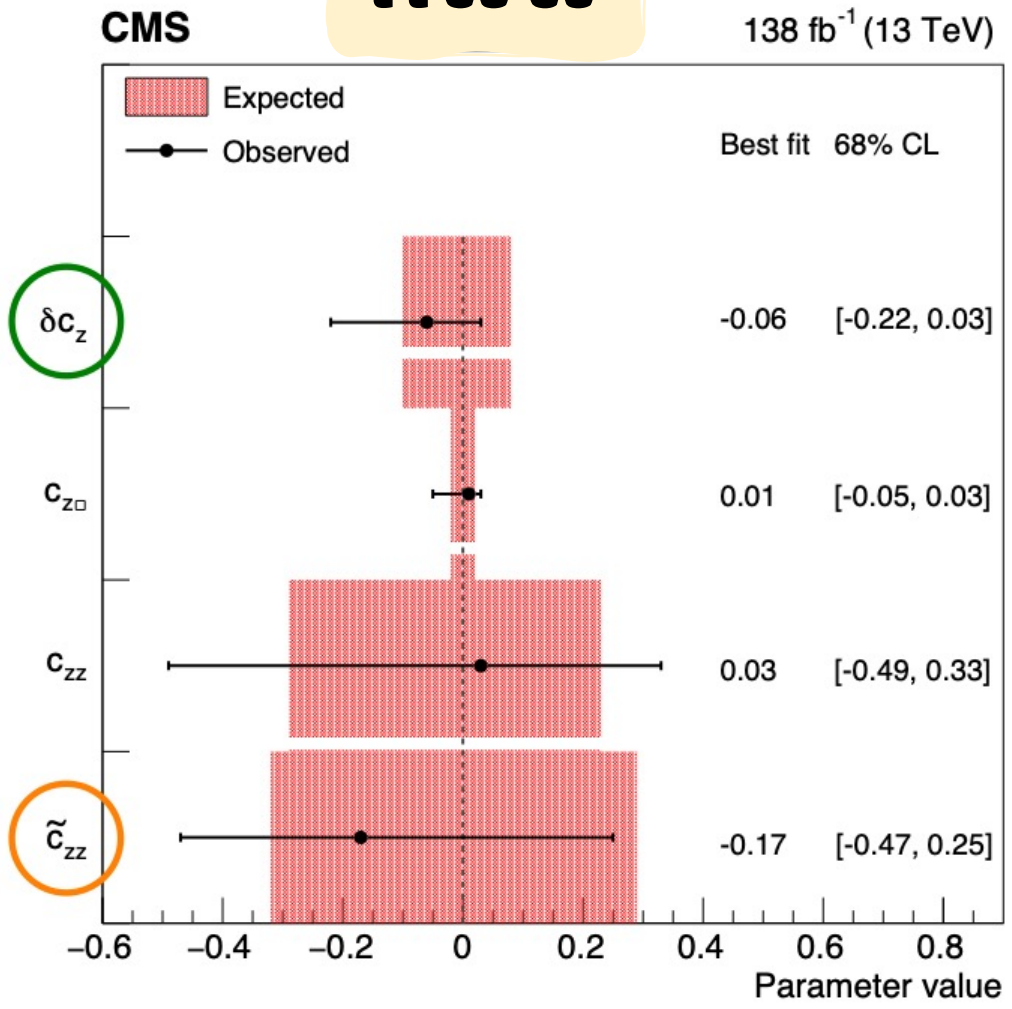
$$c_{z\Box} = \frac{m_Z^2 s_w^2}{e^2} \frac{\kappa_1^{ZZ}}{(\Lambda_1^{ZZ})^2}$$

Mass eigenbasis

HWW

HZZ

Results compatible with HZZ analysis

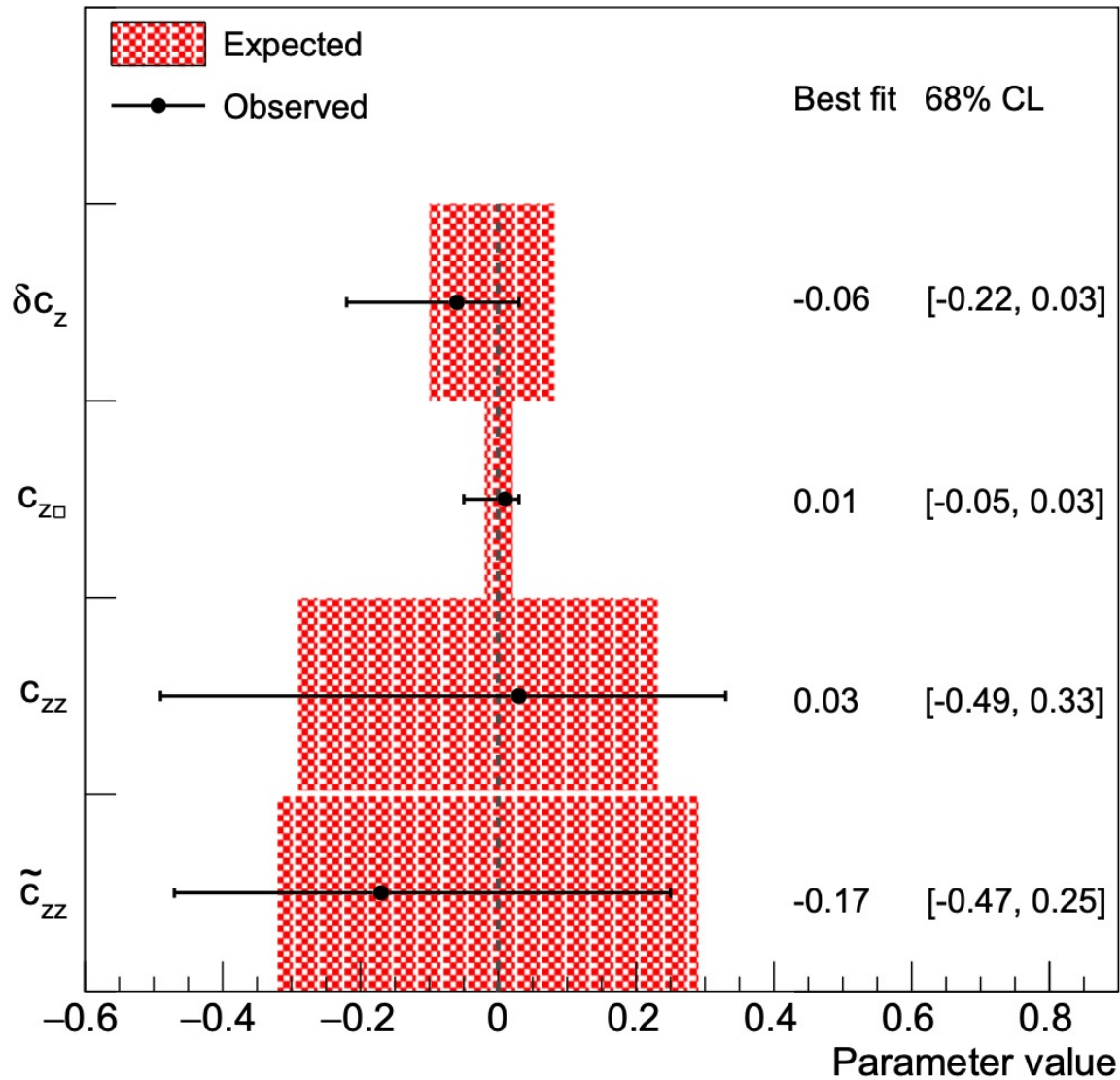


SMEFT Higgs basis

Mass eigenbasis

CMS

138 fb⁻¹ (13 TeV)



Useful for analyses combination

$$\delta c_z = \frac{1}{2} a_1^{ZZ} - 1$$

$$c_{zz} = -\frac{2s_w^2 c_w^2}{e^2} a_2^{ZZ}$$

$$\tilde{c}_{zz} = -\frac{2s_w^2 c_w^2}{e^2} a_3^{ZZ}$$

$$c_{z\Box} = \frac{m_Z^2 s_w^2}{e^2} \frac{\kappa_1^{ZZ}}{(\Lambda_1^{ZZ})^2}$$

Comparable sensitivity with full Run 2 analyses:

HZZ [PRD 104 \(2021\) 052004](#)

H $\tau\tau$ [JHEP 06 \(2022\) 012](#), [PRD 108 \(2023\) 032013](#)

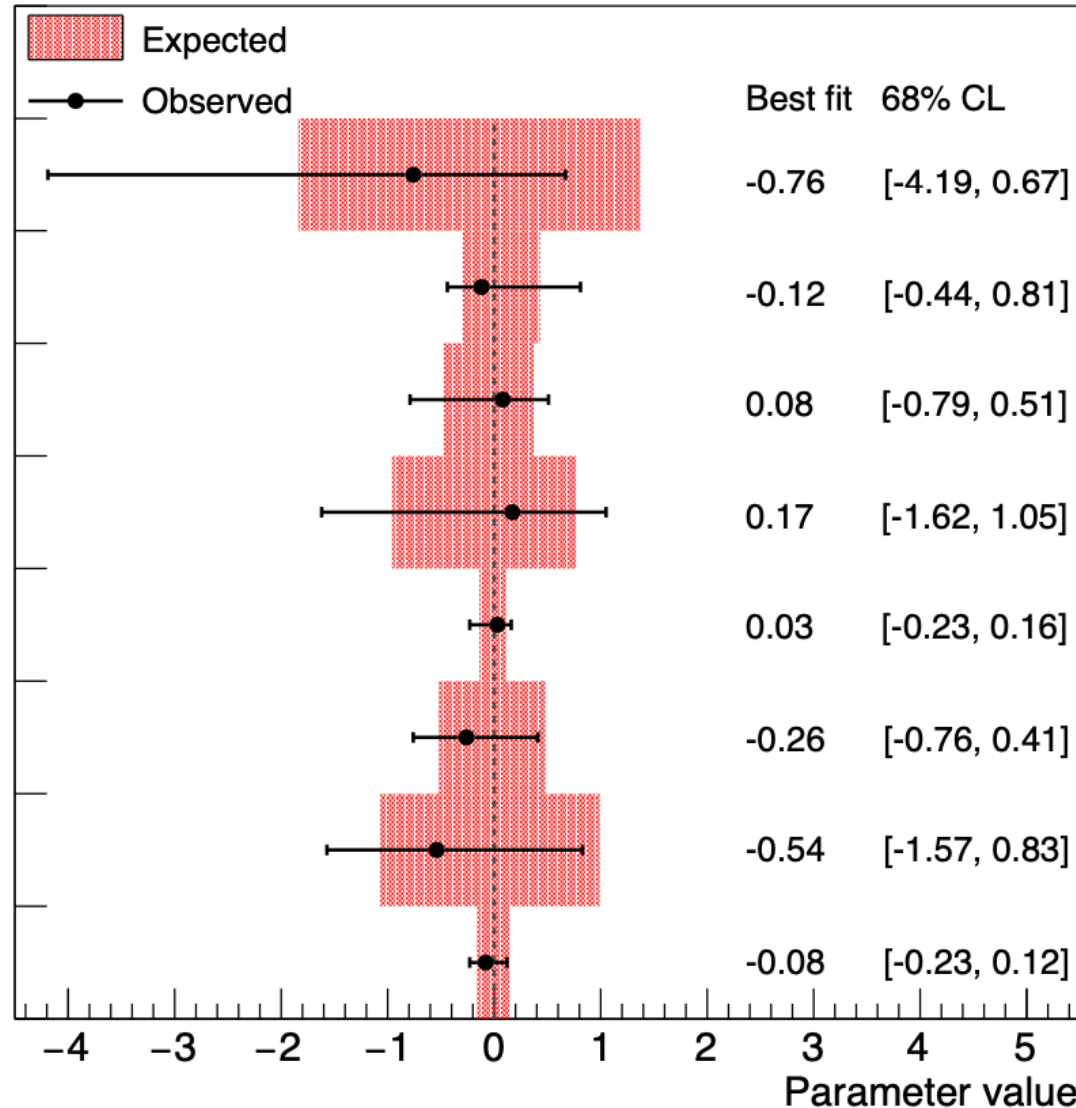
ttH analyses [JHEP 07 \(2023\) 092](#)

SMEFT Warsaw basis

Gauge eigenbasis

CMS

138 fb⁻¹ (13 TeV)



Useful for the theoretician community

$$\delta a_1^{ZZ} = \frac{v^2}{\Lambda^2} \left(2c_{H\Box} + \frac{6e^2}{s_w^2} c_{HWB} + \left(\frac{3c_w^2}{2s_w^2} - \frac{1}{2} \right) c_{HD} \right)$$

$$\kappa_1^{ZZ} = \frac{v^2}{\Lambda^2} \left(-\frac{2e^2}{s_w^2} c_{HWB} + \left(1 - \frac{1}{2s_w^2} \right) c_{HD} \right)$$

$$a_2^{ZZ} = -2 \frac{v^2}{\Lambda^2} (s_w^2 c_{HB} + c_w^2 c_{HW} + s_w c_w c_{HWB})$$

$$a_3^{ZZ} = -2 \frac{v^2}{\Lambda^2} (s_w^2 c_{H\tilde{B}} + c_w^2 c_{H\tilde{W}} + s_w c_w c_{H\tilde{W}B})$$

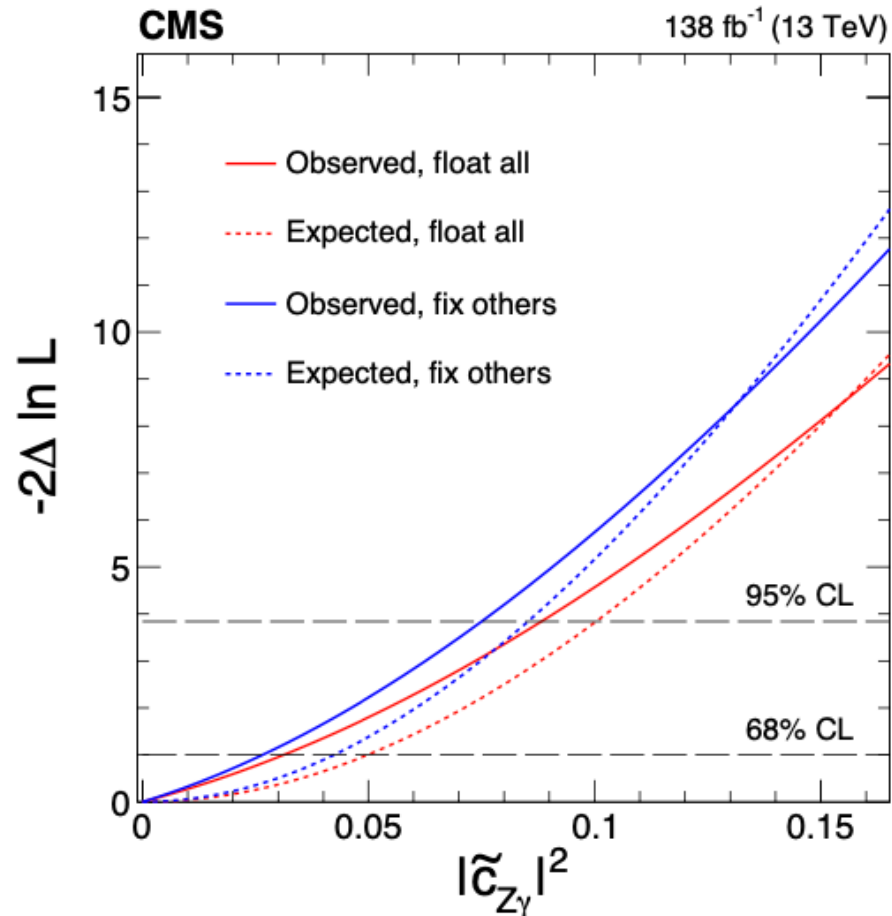
The results massively surpass that of the Run 1 analysis from the CMS experiment in both precision and coverage.

HVV couplings scans

Constraints on mass eigen basis

$$C_{\gamma\gamma}, C_{Z\gamma}, \tilde{C}_{\gamma\gamma}, \tilde{C}_{Z\gamma}$$

$H \rightarrow bb$ dominated

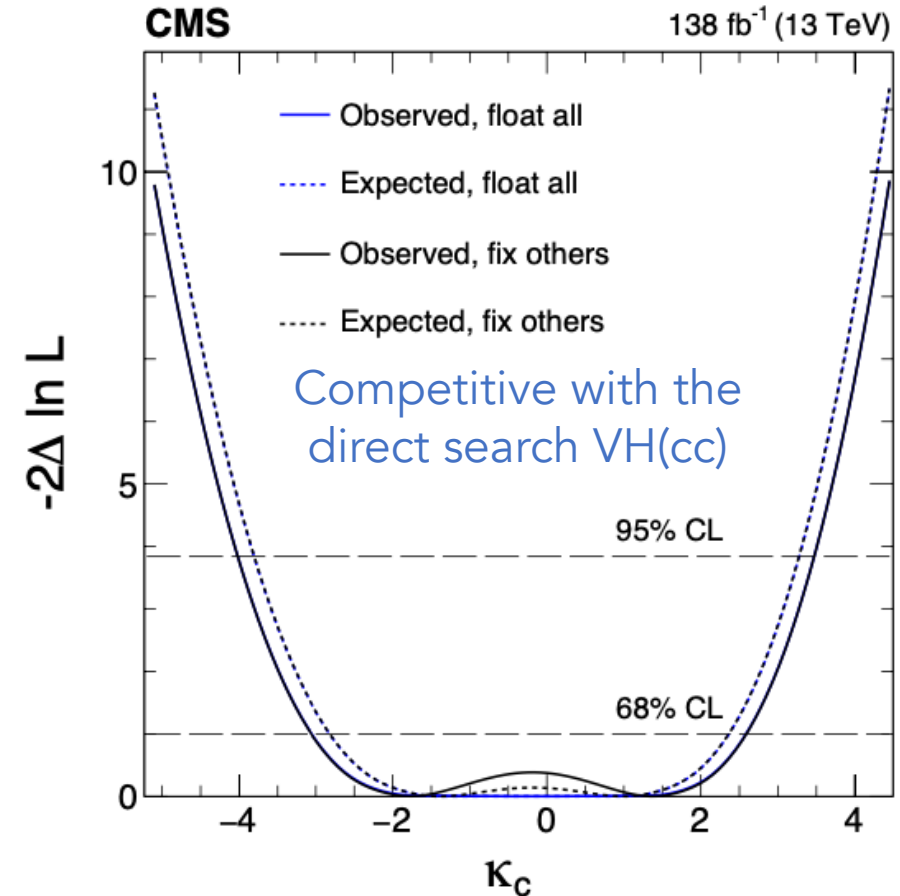


Yukawa couplings

Hff vertex parametrization

$$\kappa_u, \kappa_d, \kappa_s, \text{ and } \kappa_c$$

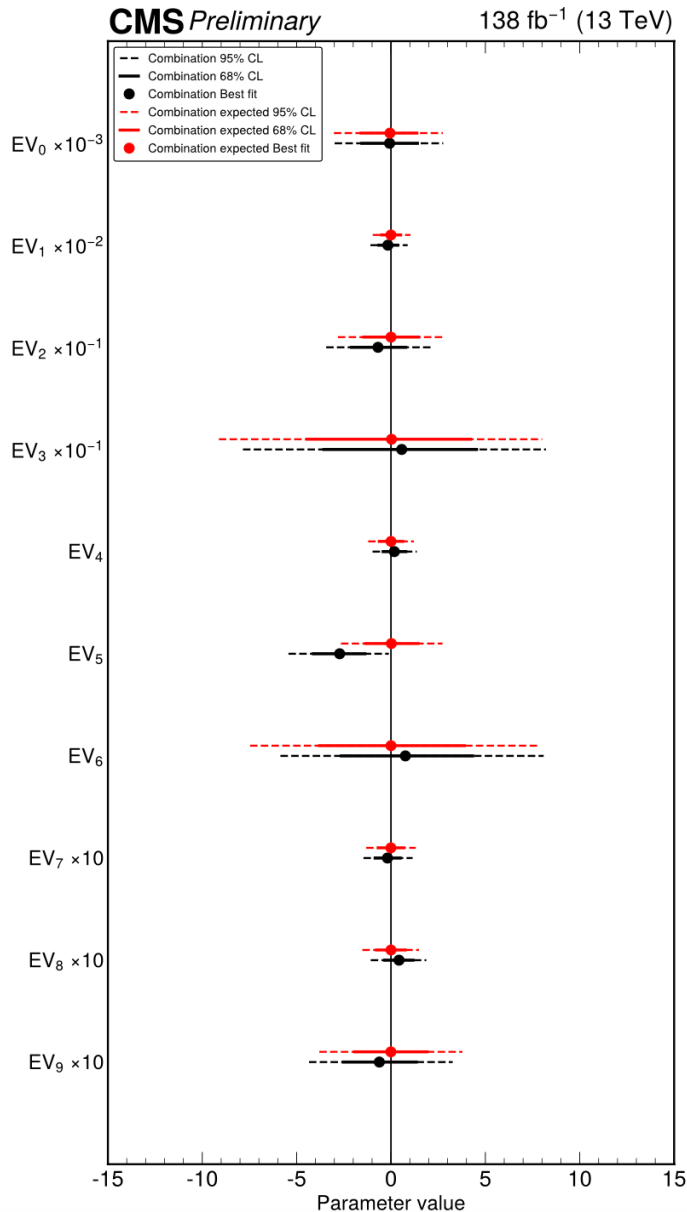
$H \rightarrow ZZ \rightarrow 4\ell$ only



Interpretation of the entire phase space

Determine linear combinations of the most constrained Wilson coefficients from the data to simultaneously constrain 10 directions in parameter space.

Results are consistent with the SM within 1σ .



CMS Preliminary 138 fb⁻¹ (13 TeV)

H → $\gamma\gamma$	0.6	66.2	5.3	7.0	20.5	0.2																									
H → ZZ	3.6		96.2			0.2																									
H → WW	2.0		97.8			0.1																									
H → $\tau\tau$	3.9		95.9			0.2																									
H → $\tau\tau$ boost	1.5		97.9			0.5																									
	Re(c_{bB})	Im(c_{bH})	Re(c_{bH})	Im(c_{bW})	Re(c_{bW})	Im(c_{eH})	Re(c_{eH})	CHB	CHbox	CHb	CHd	CHD	CHe	CHG	CHq ⁽¹⁾	CHq ⁽³⁾	CHl ⁽¹⁾	CHl ⁽³⁾	CHQ ⁽¹⁾	CHQ ⁽³⁾	CHt	CHu	CHW	CHWB	$c_{ll}^{(1)}$	Re(c_{tB})	Re(c_{tG})	Re(c_{tH})	Re(c_{tW})	Re(c_{uH})	c_W

ggH production is the most sensitive in the majority of channels

Boosted Information Tree (BIT)

Input Features:

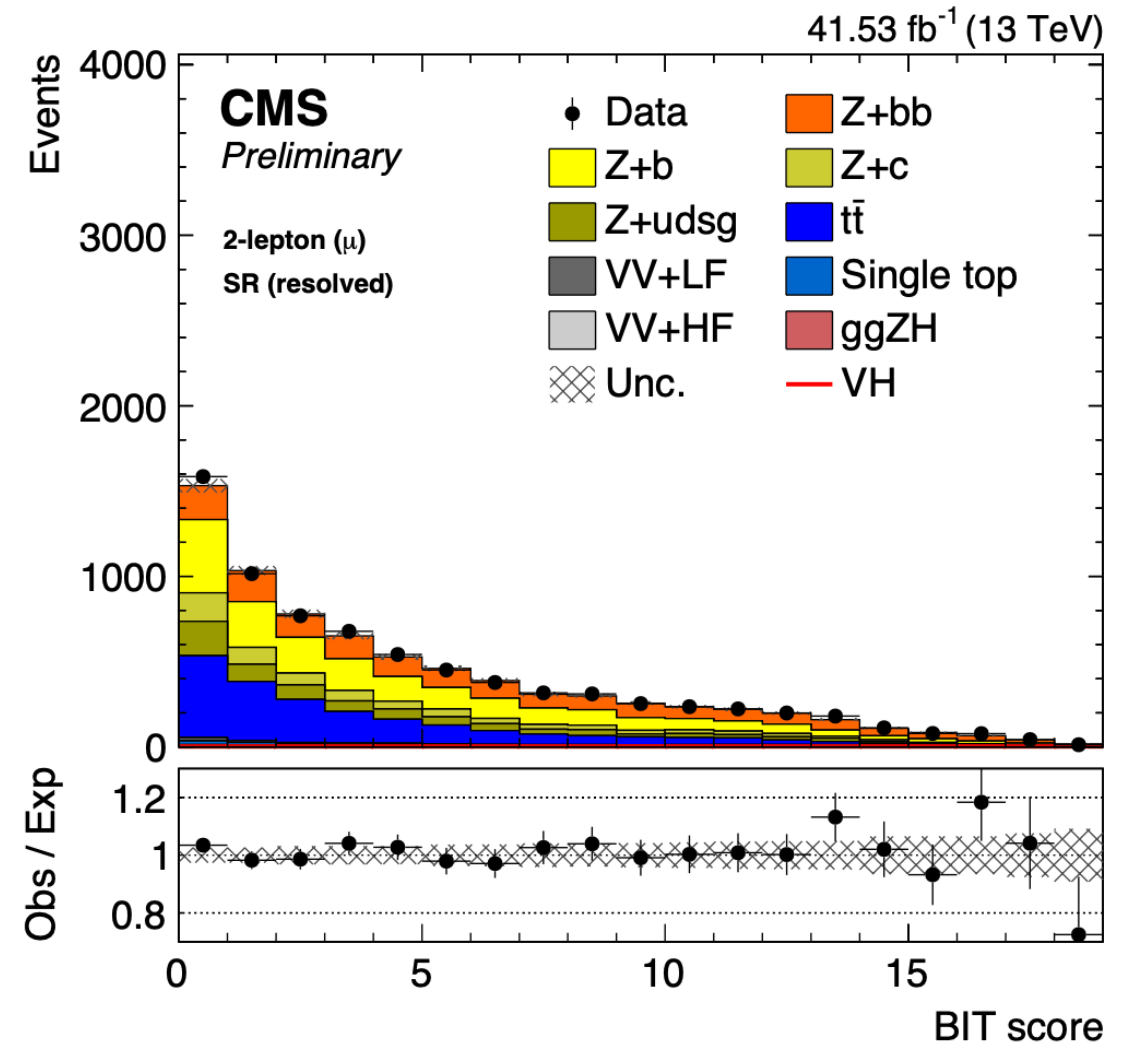
- 1- and 2-Lepton States: Angular and kinematic variables.
- 0-Lepton State: Energy-sensitive kinematic variables.

Specific Inputs

- DEEPJET: H candidate b-tagged jets
- PARTICLENET: H candidate AK8 jets

Training Procedure:

- Data: 50% for training, 50% for validation.

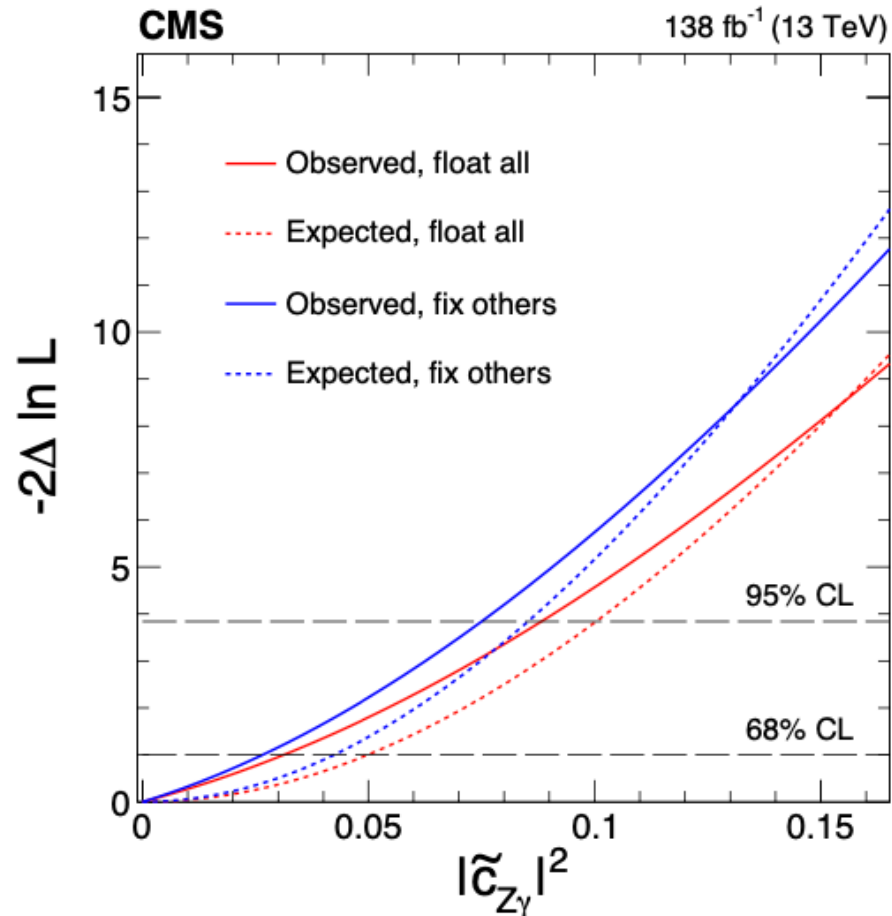


HVV couplings scans

Constraints on mass eigen basis

$$C_{\gamma\gamma}, C_{Z\gamma}, \tilde{C}_{\gamma\gamma}, \tilde{C}_{Z\gamma}$$

$H \rightarrow bb$ dominated

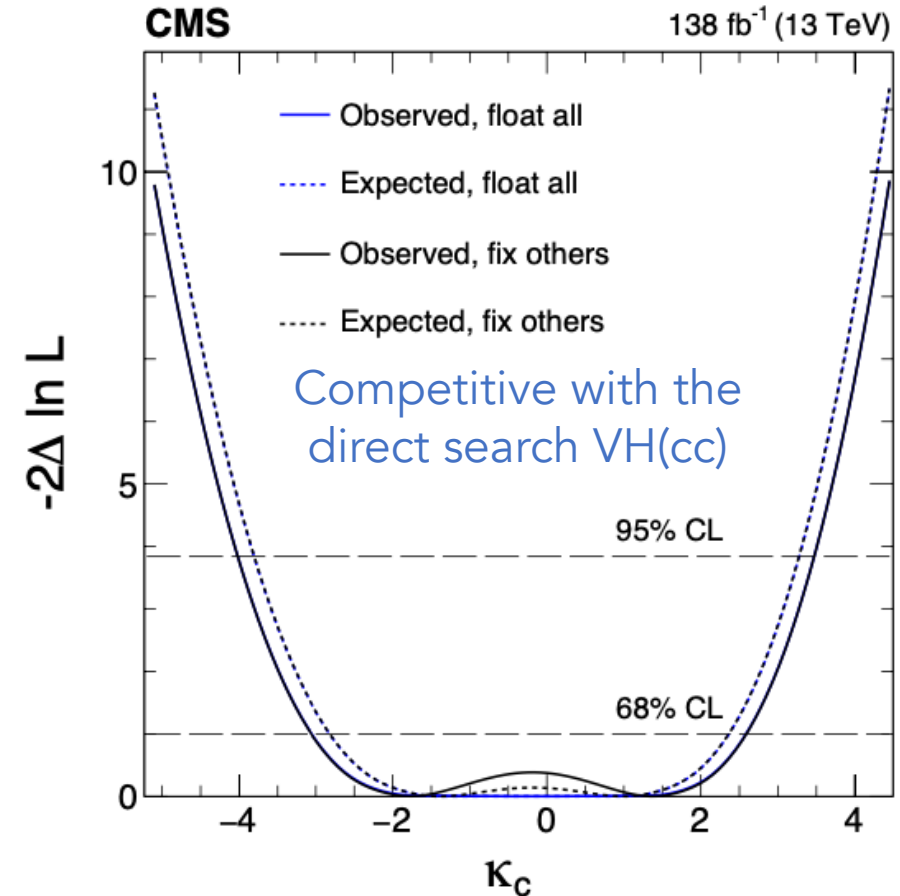


Yukawa couplings

Hff vertex parametrization

$$\kappa_u, \kappa_d, \kappa_s, \text{ and } \kappa_c$$

$H \rightarrow ZZ \rightarrow 4\ell$ only

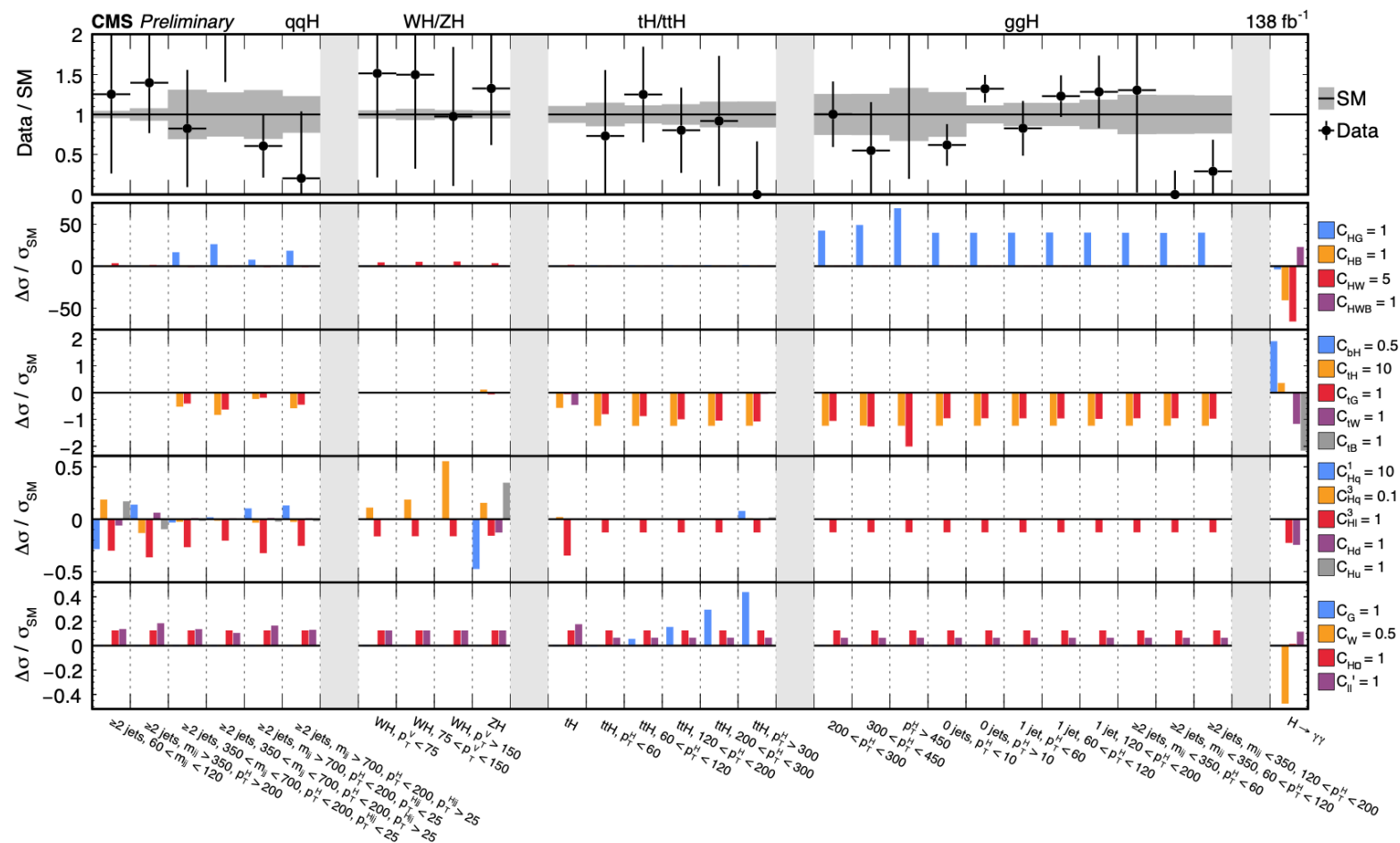


Parametrization

$$\sigma_{p,SMEFT} = \sigma_{p,SM} \left[1 + \sum \frac{A_{p,j}}{\Lambda^2} + \sum \frac{B_{p,jk}}{\Lambda^4} \right]$$

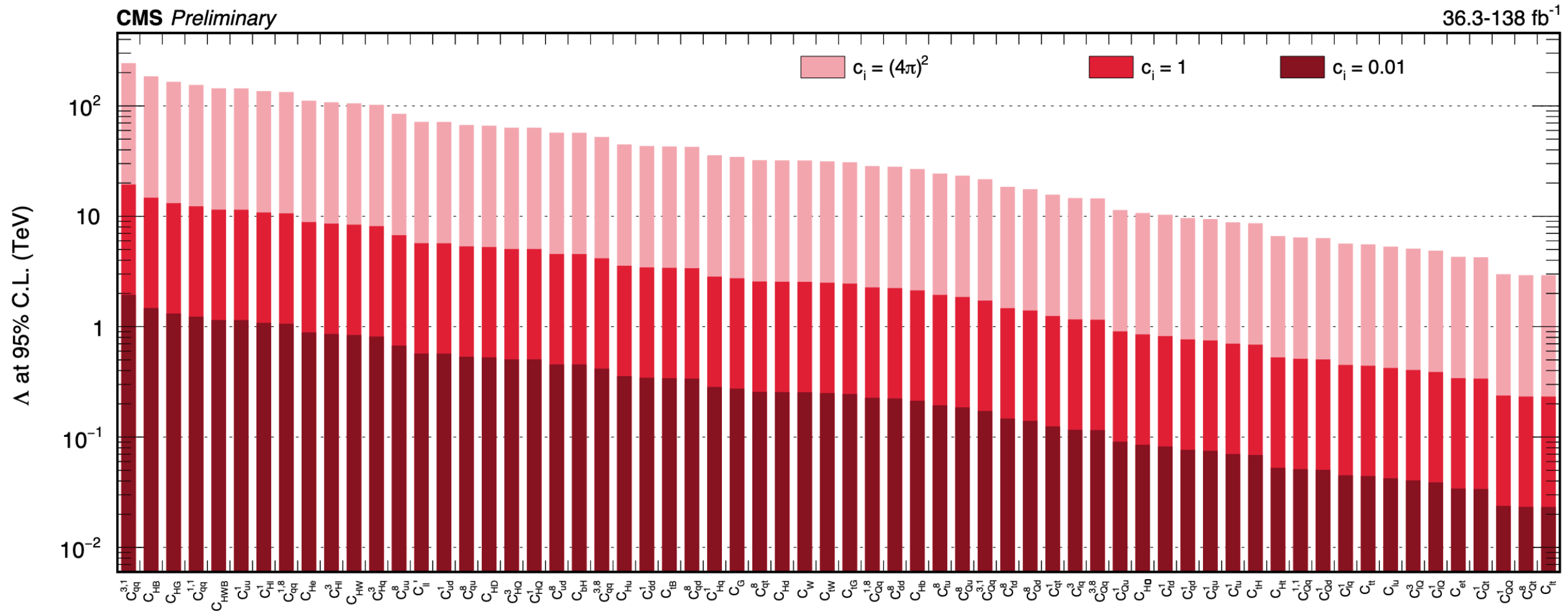
where $A_{p,j}$ and $B_{p,jk}$ represent linear and quadratic terms in the Wilson coefficients.

Impact of the linear part of parameterizations on cross sections, comparing with SM expectations.

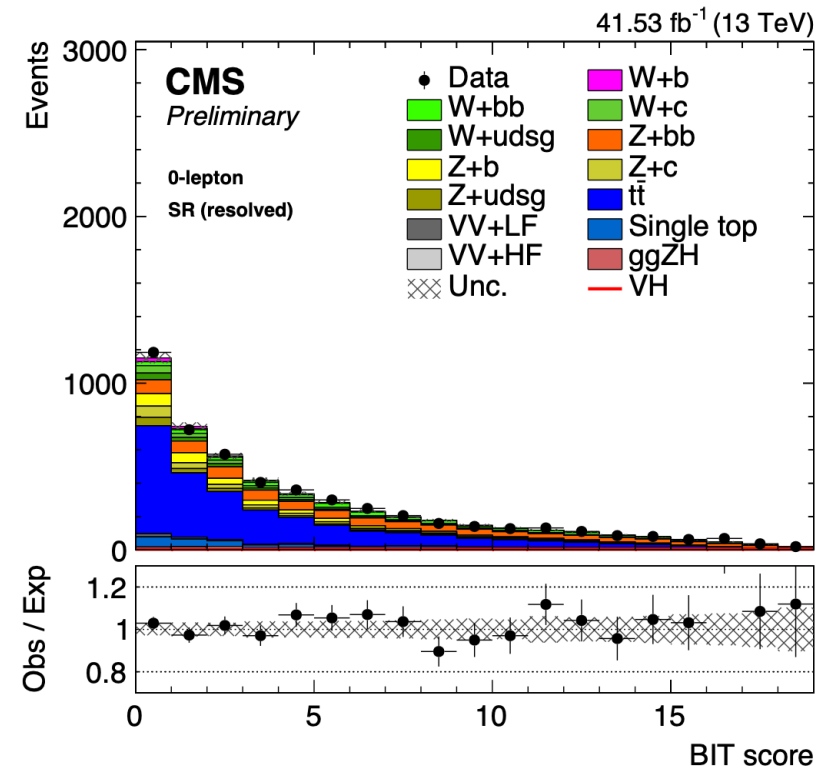
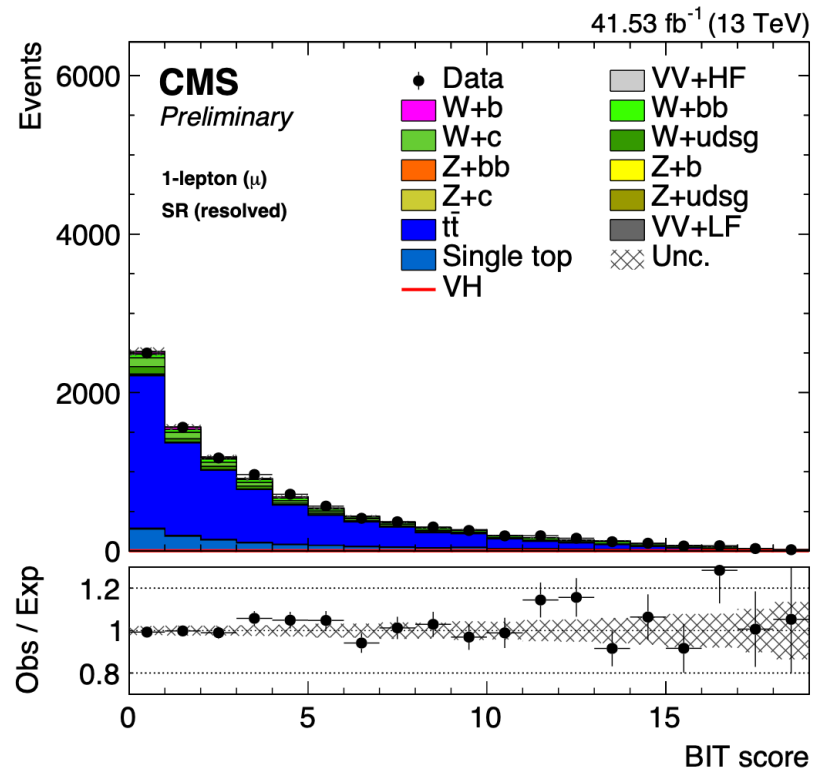
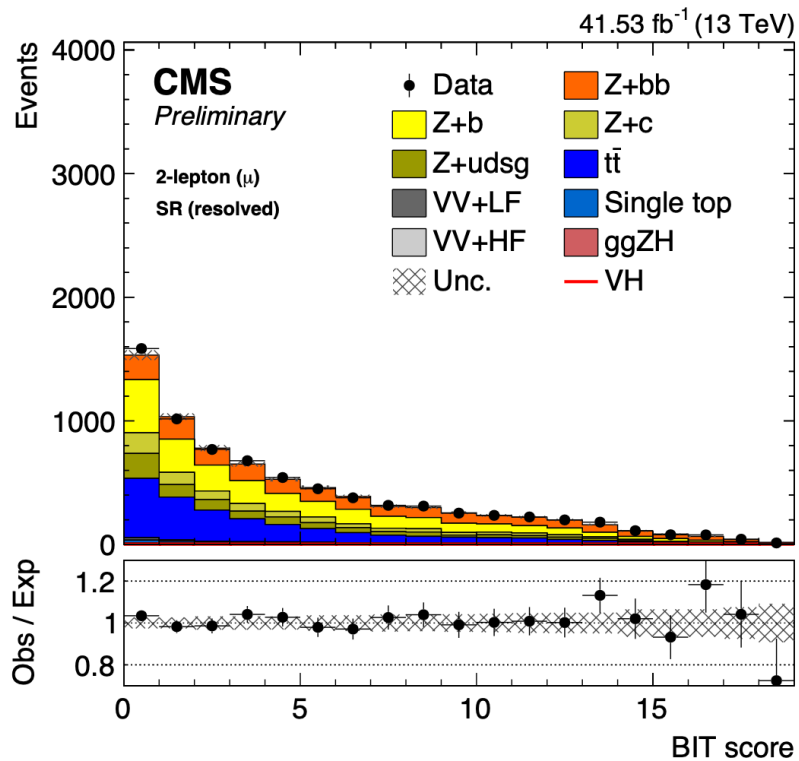


Worth Highlighting

95% CL lower limits on the scales Λ



Data/MC plots



Other Full Run 2 CMS EFT-related analyses

Presented in [HH23](#)

CMS Analysis	Channel	Measurement	Combined with	REF
HIG-19-009	On Shell $H \rightarrow ZZ$	HVV, Hgg, Htt	[Htt] $H \rightarrow \gamma\gamma$ (HIG-19-013)	PRD 104 (2021) 052004
HIG-20-006	$H \rightarrow \tau\tau$	$H\tau\tau$	-	JHEP 06 (2022) 012
HIG-20-007	$H \rightarrow \tau\tau$	HVV, Hgg, Htt	on-Shell $H \rightarrow ZZ$ + $H \rightarrow \gamma\gamma$	PRD 108 (2023) 032013
HIG-21-006	ttH and tH	Htt	on-Shell $H \rightarrow ZZ$ + $H \rightarrow \gamma\gamma$	JHEP 07 (2023) 092
HIG-21-013	off-Shell $H \rightarrow ZZ$	H Off-Shell evidence $\Gamma_{\text{Higgs}}, \text{HVV}$	on-Shell $H \rightarrow ZZ$	Nat. Phys. 18 (2022) 1329